NASA CONTRACTOR REPORT

NASA CR-2330

NASA CR-2330

ELASTIC STABILITY OF LAMINATED, FLAT AND CURVED, LONG RECTANGULAR PLATES SUBJECTED TO COMBINED INPLANE LOADS

by A. V. Viswanathan, M. Tamekuni, and L. L. Baker

Prepared by
BOEING COMMERCIAL AIRPLANE COMPANY
Seattle, Wash. 98124
for Langley Research Center

NATIONAL AERONAUTICS AND SPACE ADMINISTRATION • WASHINGTON, D. C. • JUNE 1974

1. Report No.	2. Government Accession No.	3. Recipient's Catalog No.
NASA CR-2330		

4. Title and Subtitle	5. Report Date
ELASTIC STABILITY OF LAMINATED, FLAT AND CURVED, LONG RECTANGULAR PLATES SUBJECTED TO COMBINED INPLANE LOADS	June 1974
	6. Performing Organization Code
7. Author(s)	8. Performing Organization Report No.
A. V. Viswanathan, M. Tamekuni, and L. L. Baker	D6-60227
	10. Work Unit No.
9. Performing Organization Name and Address	11. Contract or Grant No.
Boeing Commercial Airplane Company P. O. Box 3707 Seattle, Washington 98124	NAS 1-11879
	13. Type of Report and Period Covered
12. Sponsoring Agency Name and Address	Contractor report
National Aeronautics and Space Administration Washington, D.C. 20546	14. Sponsoring Agency Code

15. Supplementary Notes

Contractor program manager: Dr. Ralph E. Miller, Jr.

Final Report

16. Abstract

A method is presented to predict theoretical buckling loads of long, rectangular flat and curved laminated plates with arbitrary orientation of orthotropic axes in each lamina. The plate is subjected to combined inplane normal and shear loads. Arbitrary boundary conditions may be stipulated along the longitudinal sides of the plate. In the absence of inplane shear loads and "extensional-shear" coupling, the analysis is also applicable to finite length plates.

Numerical results are presented for curved laminated composite plates with various boundary conditions and subjected to various loadings. These results indicate some of the complexities involved in the numerical solution of the analysis for general laminates. The results also show that the "reduced bending stiffness" approximation when applied to buckling problems could lead to considerable error in some cases and therefore must be used with caution.

17. Key Words (Suggested by Author(s))		18. Distribution Statement
Stability	Combined inplane loads	Unclassified–Unlimited
Flat plates	Composites	
Curved plates		
Laminated		
		STAR Category: 32

19. Security Classif. (of this report)	20. Security Classif. (of this page)	21. No. of Pages	22. Price*
Unclassified	Unclassified	67	$3.75

*For sale by the National Technical Information Service, Springfield, Virginia 22151

CONTENTS

ELASTIC STABILITY OF LAMINATED, FLAT AND CURVED, LONG RECTANGULAR PLATES SUBJECTED TO COMBINED INPLANE LOADS

by A. V. Viswanathan, M. Tamekuni, and L. L. Baker
Boeing Commercial Airplane Company

1.0 SUMMARY

A method is presented to predict theoretical buckling loads of long, rectangular flat and curved laminated plates with arbitrary orientation of orthotropic axes in each lamina. The plate is subjected to combined inplane normal and shear loads. Arbitrary boundary conditions may be stipulated along the longitudinal sides of the plate. In the absence of inplane shear loads and "extensional-shear" coupling, the analysis is also applicable to finite length plates.

Numerical results are presented for curved laminated composite plates with various boundary conditions and subjected to various loadings. These results indicate some of the complexities involved in the numerical solution of the analysis for general laminates. The results also show that the "reduced bending stiffness" approximation when applied to buckling problems could lead to considerable error in some cases and therefore must be used with caution.

2.0 INTRODUCTION

Fiber-reinforced composite materials are finding increased applications in aerospace structures. Capability to predict the buckling behavior of thin laminated plates made from these materials, when subjected to combined inplane normal and shear loads, is of prime interest to the structural analyst. A particular characteristic of these laminated plates, in contrast to homogeneous plates, is the possible coupling between inplane extension and out-of-plane bending, references 1 and 2. Such coupling can significantly affect the load response of these plates, reference 3.

Considerable literature exists on the buckling of isotropic and orthotropic plates with various boundary conditions and subjected to various loadings. References 4 through 12 are examples of analysis for isotropic plates. Reference 13 presents an extensive treatment of orthotropic plates, where the axes of orthotropy do not coincide with the plate axes, resulting in "mixed-order derivatives" in the stability equations. A summary of this and other similar work is given in references 14 and 15.

Buckling of laminated composite plates has been receiving increased attention in the recent past. References 16 through 21 are examples of the analysis for flat plates. The phenomenon of possible bending-stretching coupling in these plates is known to have a detrimental effect and adds to the complexity of the buckling analysis. The use of "reduced bending stiffness" as formulated in references 1 and 22 has been used in conjunction with classical orthotropic plate buckling analysis, to allow for coupling effects, references 18, 20, and 21. The inplane boundary conditions do not enter into this type of analysis. These boundary conditions are known to significantly influence the buckling of flat plates in the presence of bending-stretching coupling, references 19 and 23. Therefore, caution has to be exercised in applying the "reduced bending stiffness" concept. As the number of laminas increases, the exact solution for certain types of lamina layups approaches the orthotropic plate solution, reference 3.

Few analytical results are available for laminated composite rectangular curved plates. The analysis of reference 24 may be readily applied to curved plates which are subjected to biaxial inplane normal loads and wherein no "shear-extensional" coupling is present. For such laminates, reference 25 considers the effect of the stacking sequence on buckling.

The buckling analysis presented here considers rectangular flat or curved general laminates subjected to combined inplane normal and shear loads. The analysis is applicable to (i) finite length plates, when the plate is "specially orthotropic" (i.e., "16" and "26" elements in equations (A-6) and (A-7) are zero) and the combined inplane loads do not include shear, and (ii) infinitely long

plates, for all other cases. Arbitrary boundary conditions may be specified along the sides (y = constant). See figure 1. For finite length plates, simply supported boundary conditions are stipulated along the ends (x = constant).

The method of analysis is such that it may be readily extended to longitudinally stiffened structures, subjected to combined inplane normal and shear loads, in a manner analogous to that of reference 24. A stiffness matrix is derived (from a solution of the "stability equations") relating the buckling displacements and the corresponding forces along the sides (y = constant) of the plate. The elements of this matrix are transcendental functions of the external loading and the half-wavelength of buckling, λ, in the x-direction. In general, the stiffness matrix is complex and Hermitian in form. The buckling criterion is formulated in a determinantal form, after enforcing the desired boundary conditions along the sides of the plate. For a chosen half-wavelength, λ, a buckling load is evaluated by an iteration procedure using the algorithm discussed in reference 26. Therefore a series of half-wavelengths must be investigated to determine the minimum buckling load.

The assumptions made in the analysis are:

- Small deflection theory is used.
- Effects of prebuckling deformations are ignored. At buckling the plate is in a state of uniform stresses corresponding to the external loads.
- The material is linearly elastic.

A computer program, "BUCLAP2", reference 27, based on the present analysis has been written for the CDC 6600 computer.

3.0 SYMBOLS

a	length of the plate
A_{ij}	extensional stiffnesses (i, j = 1, 2, 6), equation (A-6)
A^*	matrix for strain calculation, equation (A-56)
b	developed width of the plate
B_{ij}	stiffnesses (i, j = 1, 2, 6) associated with bending-stretching coupling, equation (A-6)
d	displacement vector
D_{ij}	bending stiffnesses (i, j = 1, 2, 6), equation (A-7)
E_{11}, E_{22}	Young's moduli of orthotropic lamina
f	force vector
G_{12}	shear modulus of orthotropic lamina
h_k	distance to k^{th} lamina from the reference plane
k_w, k_θ, k_v, k_u	spring constants
ℓ_1, ℓ_2	direction cosines
$L_1, L_2, \ldots L_6$	linear differential operators, equations (A-25) to (A-27)
$\bar{L}_{1j}, \bar{L}_{2j}$	displacement ratio coefficients, equations (A-38) and (A-39)
M_x, M_y, M_{xy}	moment resultants, equation (A-7)
$\hat{M}, \tilde{M}$	moment resultants, equations (A-18) and (A-22)
n	number of laminas

N_x, N_y, N_{xy}	stress resultants, equation (A-6)
$\bar{N}_x, \bar{N}_y, \bar{N}_{xy}$	applied inplane loads
$\hat{N}, \tilde{N}$	effective stress resultants, equations (A-19) and (A-24)
p_j	buckling displacement parameter
Q_{ij}	orthotropic material constants (i, j = 1, 2, 6) with respect to material axes, equation (A-5)
$\bar{Q}_{ij}$	orthotropic material constants (i, j = 1, 2, 6) with respect to plate axes, equation (A-3)
$\hat{Q}, \tilde{Q}$	effective transverse shears, equations (A-17) and (A-21)
r	vector of displacement coefficients, equation (A-45)
R	reference plane radius of curved plate
$R_{11}\ R_{12}, \ldots R_{33}$	elements of coefficient matrix R, equation (A-37)
RBS	reduced bending stiffness
s	stiffness matrix for the plate, equation (A-53)
S	modified merged stiffness matrix, equation (A-54)
t_k	thickness of k^{th} layer of the laminate
t	laminate thickness
$\hat{T}, \tilde{T}$	effective inplane shear, equations (A-20) and (A-23)
u, v, w	buckling displacements of the reference plane
U_j, V_j, W_j	buckling displacement coefficients, equations (A-34) through (A-36)
V_f	volume fraction

x, y, z	orthogonal coordinates
X_d, X_f	displacement and force matrices, respectively, equations (A-45) and (A-51)
α_j, β	buckling displacement parameters, equations (A-34) through (A-36)
γ_{xy}	shear strain
δ	vector corresponding to modified merged stiffness matrix, equation (A-54)
ϵ_x, ϵ_y	normal strains
θ_x, θ_y	rotations, equations (A-18) and (A-22)
κ_x, κ_y, κ_{xy}	changes in curvatures
λ	half-wavelength of buckling in the x-direction
ν_{12}, ν_{21}	Poisson's ratio
ρ	density
σ_x, σ_y	normal stresses
σ_{xy}	shear stress
ϕ_k	angle defining orthotropy directions of k^{th} lamina, with respect to plate axes

Subscripts

j	index corresponding to characteristic roots
k	layer index

A subscript preceded by a comma indicates partial differentiation with respect to the subscript.

Superscripts

T	matrix transpose
o	quantities in the reference plane of the plate
+	quantities along the side $y = +\frac{b}{2}$ of the plate
-	quantities along the side $y = -\frac{b}{2}$ of the plate

4.0 RESULTS AND DISCUSSION

The details of the buckling analysis are presented in appendix A. The numerical results from the associated computer program "BUCLAP2" were initially verified with other available results. They included both flat and curved plates with various boundary conditions and various loadings. Good correlation was obtained with results from references 4, 5, 8, 13, 15, 21, 24, and 28 through 30. These are not further discussed here. The computer program "BUCLAP2" was then used to study the buckling behavior of some laminated composite long plates. These results are discussed below. In all examples the maximum value of λ/b is limited to 250, except in cases where the variation of the buckling load with λ/b is investigated. Table 1 gives the material properties used in this study.

4.1 INFLUENCE OF CURVATURE AND INPLANE BOUNDARY CONDITIONS ON THE BUCKLING BEHAVIOR OF A LAMINATED CURVED PLATE

The cross-sectional geometry and the layup of a symmetrically laminated boron/epoxy plate are shown in figure 2. For this laminate, the stiffnesses $A_{16} = A_{26} = 0$ and all B_{ij} $(i,j = 1, 2, 6) = 0$. The various boundary conditions considered along the two sides of the plate and the corresponding codes used to designate them are also tabulated in figure 2. The buckling of the plate is investigated for these boundary conditions, when subjected to various combinations of inplane loads, with the curvature parameter $b^2/R\tilde{t}$ ranging from 1 to 1000.

The results for axial loading $\bar{N}_x$ are shown in figure 3. The numbers designating the curves correspond to the boundary condition numbers tabulated in figure 2. For this example simultaneously releasing the restraints to the inplane displacements u and v along the two sides of the plate while reducing the buckling load by 15% to 20% in the intermediate range of $b^2/R\tilde{t}$, has a very detrimental effect in the higher range of $b^2/R\tilde{t}$. The λ/b values corresponding to the buckling loads are shown in table 2.

Figure 4 shows the variation of the buckling load with respect to λ/b, for the various boundary conditions, when the plate with $b^2/R\tilde{t} = 300$ is subjected to transverse loading $\bar{N}_y$. The curves show a general trend of nearly reaching an asymptotic buckling load in the region of the "humps", followed by a marked drop in the buckling load with further increase in λ/b. It is thought that a change in buckle mode is possibly associated with each "hump" region. It is feasible to verify this by obtaining eigenvector solutions corresponding to buckling loads, which was not done here.

A comparison of the different curves in figure 4 shows the significance of the inplane boundary conditions, in particular the restraint to the v displacement. For boundary condition

code uN_y (BC-uN_y) the results obtained from using Donnell-type stability equations are also shown in the figure. They deviate significantly from the results of the present analysis for high λ/b values.

The results for BC-uN_y further show that the buckling load is continuing to decrease in the region of $\lambda/b = 250$. Perhaps this is the little significance, since plates of such high aspect ratio are not used in practical structures. However, the "humps" in the curves are indicative of the care necessary in interpreting the results when an upper limit of λ/b is arbitrarily chosen. Figure 5 shows the plot of λ/b versus $\bar{N}_y$ when $b^2/R\tilde{t} = 1.0$ (i.e., a nearly flat plate) for BC-N_yN_{xy}. A sharp drop in the buckling load is noticed in the region of $\lambda/b \approx 100$, perhaps caused by a change in the buckling mode.

The variation of the buckling load $\bar{N}_y$ with the change in curvature parameter $b^2/R\tilde{t}$ is shown in figure 6 for various boundary conditions. These results are based on an upper limit of 250 for λ/b. As seen earlier in figure 4, for the plate with $b^2/R\tilde{t} = 300$ the buckling loads for BC-uN_y could drop down to that for BC-N_yN_{xy} at higher values of λ/b. Thus, with a higher cutoff for λ/b, the curve for BC-uN_y in figure 6 would drop down to that of BC-N_yN_{xy} in the higher range of $b^2/R\tilde{t}$ values. In any case, the results show the significance of the inplane boundary conditions. Further, for this example, the curves have an intermediate region where the buckling load varies very little with respect to $b^2/R\tilde{t}$. These results are also given in table 3.

The next loading considered is the inplane shear $\bar{N}_{xy}$. The plot of $\bar{N}_{xy}$ versus λ/b, for a plate with $b^2/R\tilde{t} = 700$ and BC-uN_y is shown in figure 7. The two minimums seen indicate that one has to be cautious in choosing the λ/b range to be investigated in order to establish the minimum buckling load. Figure 8 shows the change in the buckling load with respect to $b^2/R\tilde{t}$, for various boundary conditions. The corresponding λ/b values are given in table 4. It is observed that, with some exceptions, the λ/b values are in general small and thus point to the first minimum seen in figure 7. Boundary conditions uN_y and $N_{xy}N_y$ are essentially the same as BC-uN_y and N_yN_{xy}, with the inplane displacement v completely restrained along one side of the plate. Figure 8 indicates that such a restraint raises the curves for BC-uN_y and N_yN_{xy} to the level of those for BC-uv and vN_{xy}. From this it may be conjectured that at high $b^2/R\tilde{t}$ values the buckling modes corresponding to BC-uN_y and N_yN_{xy} involve large inplane displacements. It is pointed out that the use of the "engineering strain" as given by equations (A-11) through (A-13) in deriving the stability equations (A-14) through (A-16) permits such buckling modes.

The theoretical buckling loads for the combined loading of $\bar{N}_x$ and $\bar{N}_{xy}$ with $\bar{N}_x = \bar{N}_{xy}$ are plotted in figure 9, for $b^2/R\tilde{t}$ ranging from 1.0 to 1000 and for various boundary conditions. The corresponding λ/b values are given in table 5. These results indicate considerable reduction in the buckling load compared to the individual load case results in tables 2 and 4. A closer study of the results in the latter tables, for high $b^2/R\tilde{t}$ values, shows that this laminate has a much lower critical load in shear ($\bar{N}_{xy}$) than in axial compression ($\bar{N}_x$). Thus, for the combined load case of $\bar{N}_{xy} = \bar{N}_x$,

the shear load $\bar{N}_{xy}$ may be expected to govern the laminate behavior at high $b^2/R\tilde{t}$ values. This is confirmed by the striking similarity between figures 8 and 9.

Similar results for other combined load cases of $\bar{N}_y = \bar{N}_{xy}$, $\bar{N}_y = \bar{N}_x$, and $\bar{N}_x = \bar{N}_y = \bar{N}_{xy}$ are shown in figures 10, 11, and 12, respectively (and in tables 6, 7, and 8, respectively). For all these loading cases and at most $b^2/R\tilde{t}$ values the laminate has a much lower critical load in transverse compression ($\bar{N}_y$) than in axial compression ($\bar{N}_x$) or shear ($\bar{N}_{xy}$). Thus the results for the above-mentioned combined load cases show the same trend as the results for the $\bar{N}_y$ loading case in figure 6. In this respect, a more appropriate choice of the loading ratios for these combined load cases would have better indicated the interaction effects.

4.2 BUCKLING OF CURVED LAMINATES WITH INCREASING NUMBER OF LAYERS

Figure 13 shows the cross section of a curved laminate. The sides along A and B are simply supported. The laminate is built up from alternating layers of +45° and -45°. As the number of layers is increased, the laminate is symmetric for odd numbers of layers ($B_{ij} = 0$) and is antisymmetric for even numbers of layers ($A_{16} = A_{26} = D_{16} = D_{26} = B_{11} = B_{22} = B_{12} = 0$). Theoretical buckling loads for the load cases $\bar{N}_x$ only, $\bar{N}_y$ only, $\bar{N}_{xy}$ only, and $\bar{N}_x = \bar{N}_{xy}$ are given in table 9 and figure 14 for odd numbers of layers and in table 10 and figure 15 for even numbers of layers, as the number of layers is increased from 1 to 15. The results in these tables designated "16, 26 = 0" are obtained by setting to zero the "16" and "26" elements in equations (A-6) and (A-7). A comparison of the results for odd numbers of layers in table 9 shows that the presence of the A_{16}, A_{26}, D_{16}, and D_{26} terms for the laminate considered increases the buckling load by about 10% for the load cases N_{xy} only and $N_{xy} = N_x$. This increase can be attributed to the significance of the shear stress direction in buckling of fiber-reinforced composites, as pointed out in reference 3.

The results in table 10 for even numbers of layers (antisymmetric laminates) show that the presence of B_{16} and B_{26} causes a reduction in the buckling load for all load cases considered. However, as the number of layers increases, this reduction becomes insignificant.

The "reduced bending stiffness" (RBS) approximation, references 1 and 22, was applied to the antisymmetric laminates considered here. The corresponding results are also given in table 10. They show that the RBS approximation is valid for these examples. The validity of the RBS approximation is further considered in Section 4.4. Some of the results from tables 9 and 10 are plotted in figures 14 and 15.

4.3 EFFECT OF FIBER ANGLE ON SHEAR BUCKLING OF A CURVED LAMINATE FOR FOUR DIFFERENT COMPOSITE SYSTEMS

Figure 16 shows the cross-sectional geometry of a curved laminate, the fiber directions being the same in all layers. One side of the plate is clamped; the other side is simply supported. The equivalent weight thicknesses of the four composite systems considered, together with that for 2024 aluminum alloy, are also tabulated in figure 16. The results for the shear buckling load $\bar{N}_{xy}$ as the fiber angle is varied from -90° to +90° are shown in figure 17. Also shown are the results for the equivalent weight aluminum curved plate and a similar boron/epoxy flat plate.

The boron/epoxy and the graphite/epoxy systems appear to be more sensitive to the fiber angle than the boron/aluminum or borsic/aluminum systems. This behavior may be attributed to the large differences in the E_{11}/G_{12} ratios. In relation to the boron/epoxy curved plate the corresponding graphite/epoxy plate is seen to be superior at all fiber angles, based on resistance to shear buckling. This is due to the higher modulus/density ratio of the graphite/epoxy system. It is interesting to note that at small fiber angles the critical loads for the two epoxy systems fall below that for aluminum. The boron/aluminum and the borsic/aluminum plates are seen to be superior in the intermediate range of fiber angles. A comparison of the results for the flat and curved boron/epoxy plates indicates that the optimum fiber angle can be expected to be a function of curvature.

Figure 18 shows the variation of $\bar{N}_{xy}$ with respect to half-wave length for some fiber angles in the graphite/epoxy system considered above. These curves, in general, show two relative minimum buckling loads at different half-wave lengths, as previously noted in figure 7. It is seen that the absolute minimum buckling load at $\phi = 15°$ corresponds to the first relative minimum, whereas at $\phi = 30°$ the absolute minimum corresponds to the second relative minimum. It is therefore reasonable to expect a fiber angle between 15° and 30° at which the two relative minimums have the same buckling load. A study of the other curves in figure 18 indicates similar behavior at more than one fiber angle. Hence, for the curved laminate of figure 16, a plot of the half-wave length corresponding to the absolute minimum buckling load versus fiber angle can be expected to have discontinuities at the above-mentioned fiber angles. The results for a simply supported flat plywood plate presented in figure 40 of reference 13 do not show such discontinuities.

The effect of the fiber angle on the shear buckling of angle ply curved laminates is considered next. Boron/epoxy and boron/aluminum composite systems are chosen for this study. The laminates have four layers and are symmetric, $[+\phi/-\phi]_s$. The basic geometry and the equivalent weight thicknesses of the curved plates are as shown in figure 16. The sides A and B are either both clamped or both simply supported. Shear buckling loads $\bar{N}_{xy}$ as ϕ is varied from -90° to +90° are

shown in figure 19. The corresponding results for the boron/epoxy flat plate are also shown for comparison. The results show the same basic trend as in figure 17. If the total number of layers is increased while keeping the angle ply layup symmetric and also the total thickness constant, the curves can be expected to become symmetric with respect to $\phi = 0^\circ$

4.4 A STUDY OF SOME SIMPLIFYING ASSUMPTIONS FOR COUPLING EFFECTS IN LAMINATES

A general laminate exhibits bending-stretching coupling and shear-extension coupling. Such coupling effects not only add to the complexity of the buckling analysis, but also affect the buckling characteristics of the plate. "Reduced bending stiffness" (RBS) approximation, (refs. 1 and 22) has been often used to allow for the bending-stretching coupling effects. For the type of laminates considered in Section 4.2, the use of RBS is seen to be satisfactory. No approximation has been suggested in literature to allow for shear-extension coupling.

The above coupling effects and the use of the RBS are now further investigated. The general curved laminate shown in figure 20 consists of 0.051-cm-thick aluminum sheet (2024) reinforced on one side only with alternate layers of $+45^\circ$ and -45° boron/epoxy composite. Such a laminate exhibits full coupling effects. The buckling loads as the number of composite layers is increased in pairs of $+45^\circ/-45^\circ$ and when subjected to individual loads of $\overline{N}_x$, $\overline{N}_y$ and $\overline{N}_{xy}$ are shown in figures 21, 22, and 23, respectively, by the curves marked "exact". The figures also show the buckling loads obtained from using the following approximations, individually:

1) RBS—"Reduced bending stiffness" to allow for bending-stretching coupling

2) "16" and "26" = 0—Ignoring shear-extension coupling while retaining any bending-stretching coupling, i.e., $A_{16} = A_{26} = B_{16} = B_{26} = D_{16} = D_{26} = 0$

3) $B_{ij} = 0$—Ignoring completely bending-stretching coupling only i.e., $B_{11} = B_{22} = B_{66} = B_{12} = B_{16} = B_{26} = 0$

It is seen that the results from the second approximation (i.e., "16" and "26" = 0) are fairly close to the "exact" solution except for the shear loading $\overline{N}_{xy}$. For the latter case, the error is of the order of 5% above the "exact" solution. The RBS approximation results are about 20% higher for $\overline{N}_x$ loading, about 6% lower for the $\overline{N}_y$ loading, and about 10% higher for the $\overline{N}_{xy}$ loading, in comparison with the "exact" solution. For the laminate considered, the $B_{ij} = 0$ approximation while yielding reasonable results for the $\overline{N}_y$ loading is seen to have maximum error for the $\overline{N}_x$ and $\overline{N}_{xy}$ loadings.

In order to study a combined load case, the general curved laminate shown in figure 20 with three pairs of +45°/-45° boron/epoxy composite reinforcement is considered. The laminate is subjected to combined loads of $\bar{N}_x$ and $\bar{N}_{xy}$. The results are presented in figure 24 in the form of an interaction curve. $\bar{N}_{xo}$ and $\bar{N}_{xyo}$ are the buckling loads when these loads are acting individually. The curves clearly show the difference between the three approximations and the "exact" solution. The latter interaction curve is seen to be closely represented by the interaction equation given in reference 10, namely,

$$\left(\frac{\bar{N}_{xy}}{\bar{N}_{xyo}}\right)^2 + \frac{\bar{N}_x}{\bar{N}_{xo}} = 1$$

The results discussed indicate that all the three approximations considered, in general, predict buckling loads differing from the "exact" solution. Neglecting shear-extension coupling appears to involve minimum error. The results also indicate that the RBS approximation could lead to considerable error in certain buckling problems. In the light of the results presented, further detailed study is warranted.

5.0 CONCLUDING REMARKS

A method has been presented to predict theoretical buckling loads of long, rectangular flat and curved laminated plates with arbitrary orientation of orthotropic axes in each lamina. The plate can be subjected to combined inplane normal and shear stresses. The longitudinal sides of the plate can be arbitrarily restrained. In the absence of the inplane shear loads and the "extensional-shear" coupling, the analysis is also applicable to finite length plates.

Few results are available in the literature for laminated curved plates. Thus, the analysis presented here together with the associated computer program BUCLAP2 is expected to aid in achieving a better understanding of the buckling behavior of these curved plates, in addition to supplementing the available results for laminated flat plates.

Some results are presented for curved laminates. These indicate the complexity of the numerical solution of the buckling analysis for general laminates and the care needed in choosing the λ/b range to determine the minimum buckling load. They also indicate that an eigenvector solution to determine the buckle mode would have been useful in answering some of the questions raised by the analytical results.

The analysis has been used to make a preliminary study of the efficiency of curved plates in buckling made from various fiber-reinforced composite systems, when subjected to inplane shear loads. Results of a study of some simplifying assumptions for coupling effects in general laminates are also presented.

APPENDIX A

DETAILS OF THE ANALYSIS

This appendix describes the method used in the elastic stability analysis of curved and flat laminated rectangular plates subjected to combined inplane normal and shear loads. The equations given are for the laminated curved plate. They readily degenerate to those of the flat plate when the curvature becomes zero (infinite radius).

A.1 BASIC EQUATIONS FOR THE LAMINATE

The curved laminate considered here has constant curvature with zero Gaussian curvature. Figure 25 shows the basic geometry and sign conventions. The x-, y-, and z-axes are the structural axes of the laminate, the x- and y-axes being parallel to the sides of the plate. Each lamina is orthotropic with respect to axes 1, 2, and 3. The orthotropy directions for lamina k are defined by the angle ϕ_k between the axes x and 1, measured positive in the clockwise direction from the x-axis. In general, ϕ_k could vary from lamina to lamina. For fiber-reinforced composites, ϕ_k, as defined above, is the fiber angle of the k^{th} lamina. The midplane of the laminate is chosen as the reference plane. The strains and curvature changes in this plane, in terms of its displacements u, v, and w, are (ref. 31):

$$
\begin{aligned}
\epsilon^{\circ}_{x} &= u_{,x} \\
\epsilon^{\circ}_{y} &= v_{,y} - \frac{w}{R} \\
\gamma^{\circ}_{xy} &= u_{,y} + v_{,x} \\
\kappa^{\circ}_{x} &= - w_{,xx} \\
\kappa^{\circ}_{y} &= - w_{,yy} - \frac{1}{R} v_{,y} \\
\kappa^{\circ}_{xy} &= - 2w_{,xy} - \frac{2}{R} v_{,x}
\end{aligned}
\qquad \text{(A-1)}
$$

The radius R is measured from the reference plane to the center of curvature and is positive when in the positive direction of the z-axis, as in figure 25. By the Kirchhoff-Love hypothesis, the strains in any place distance z from the reference plane are:

$$\begin{Bmatrix} \epsilon_x \\ \epsilon_y \\ \gamma_{xy} \end{Bmatrix} = \begin{Bmatrix} \epsilon^\circ_x \\ \epsilon^\circ_y \\ \gamma^\circ_{xy} \end{Bmatrix} + z \begin{Bmatrix} \kappa^\circ_x \\ \kappa^\circ_y \\ \kappa^\circ_{xy} \end{Bmatrix} \tag{A-2}$$

The stress-strain equations for a lamina are (ref. 32):

$$\begin{Bmatrix} \sigma_x \\ \sigma_y \\ \sigma_{xy} \end{Bmatrix}_k = \begin{bmatrix} \overline{Q}_{11} & \overline{Q}_{12} & \overline{Q}_{16} \\ \overline{Q}_{12} & \overline{Q}_{22} & \overline{Q}_{26} \\ \overline{Q}_{16} & \overline{Q}_{26} & \overline{Q}_{66} \end{bmatrix}_k \begin{Bmatrix} \epsilon_x \\ \epsilon_y \\ \gamma_{xy} \end{Bmatrix}_k \tag{A-3}$$

The lamina stiffnesses $\overline{Q}_{ij}$ (i, j = 1, 2, 6), which are with respect to the axes x, y, and z, may be readily obtained from the corresponding lamina stiffnesses Q_{ij} with respect to the orthotropic axes 1, 2, and 3. The details are to be found in reference 32. The resulting equations are:

$$\begin{aligned}
\overline{Q}_{11} &= Q_{11}\ell_1^4 + 2(Q_{12} + 2Q_{66})\,\ell_1^2\ell_2^2 + Q_{22}\ell_2^4 \\
\overline{Q}_{22} &= Q_{11}\ell_2^4 + 2(Q_{12} + 2Q_{66})\,\ell_1^2\ell_2^2 + Q_{22}\ell_1^4 \\
\overline{Q}_{12} &= (Q_{11} + Q_{22} - 4Q_{66})\,\ell_1^2\ell_2^2 + Q_{12}\,(\ell_1^4 + \ell_2^4) \\
\overline{Q}_{66} &= (Q_{11} + Q_{22} - 2Q_{12} - 2Q_{66})\,\ell_1^2\ell_2^2 + Q_{66}\,(\ell_1^4 + \ell_2^4) \\
\overline{Q}_{16} &= (Q_{11} - Q_{12} - 2Q_{66})\,\ell_1^3\ell_2 + (Q_{12} - Q_{22} + 2Q_{66})\,\ell_1\ell_2^3 \\
\overline{Q}_{26} &= (Q_{11} - Q_{12} - 2Q_{66})\,\ell_1\ell_2^3 + (Q_{12} - Q_{22} + 2Q_{66})\,\ell_1^3\ell_2
\end{aligned} \tag{A-4}$$

where $\ell_1 = \cos \phi_k$, $\ell_2 = \sin \phi_k$, and

$$Q_{11} = \left[E_{11}/(1 - \nu_{21}\nu_{12})\right]_k$$

$$Q_{22} = \left[E_{22}/(1 - \nu_{21}\nu_{12})\right]_k$$

$$Q_{12} = \left[\nu_{21}E_{11}/(1 - \nu_{21}\nu_{12})\right]_k = \left[\nu_{12}E_{22}/(1 - \nu_{21}\nu_{12})\right]_k \qquad \text{(A-5)}$$

$$Q_{66} = \left[G_{12}\right]_k$$

The stress resultants N and the moment resultants M in the reference plane are written as:

$$\begin{Bmatrix} N_x \\ N_y \\ N_{xy} \end{Bmatrix} = \begin{bmatrix} A_{11} & A_{12} & A_{16} \\ A_{12} & A_{22} & A_{26} \\ A_{16} & A_{26} & A_{66} \end{bmatrix} \begin{Bmatrix} \epsilon^\circ_x \\ \epsilon^\circ_y \\ \gamma^\circ_{xy} \end{Bmatrix} + \begin{bmatrix} B_{11} & B_{12} & B_{16} \\ B_{12} & B_{22} & B_{26} \\ B_{16} & B_{26} & B_{66} \end{bmatrix} \begin{Bmatrix} \kappa^\circ_x \\ \kappa^\circ_y \\ \kappa^\circ_{xy} \end{Bmatrix} \qquad \text{(A-6)}$$

$$\begin{Bmatrix} M_x \\ M_y \\ M_{xy} \end{Bmatrix} = \begin{bmatrix} B_{11} & B_{12} & B_{16} \\ B_{12} & B_{22} & B_{26} \\ B_{16} & B_{26} & B_{66} \end{bmatrix} \begin{Bmatrix} \epsilon^\circ_x \\ \epsilon^\circ_y \\ \gamma^\circ_{xy} \end{Bmatrix} + \begin{bmatrix} D_{11} & D_{12} & D_{16} \\ D_{12} & D_{22} & D_{26} \\ D_{16} & D_{26} & D_{66} \end{bmatrix} \begin{Bmatrix} \kappa^\circ_x \\ \kappa^\circ_y \\ \kappa^\circ_{xy} \end{Bmatrix} \qquad \text{(A-7)}$$

The elements of the A, B, and D coefficient matrices are (ref. 32):

$$A_{ij} = \sum_{k=1}^{n} (\bar{Q}_{ij})_k t_k \qquad \text{(A-8)}$$

$$B_{ij} = \frac{1}{2} \sum_{k=1}^{n} (\bar{Q}_{ij})_k (h_{k+1} + h_k) t_k \qquad \text{(A-9)}$$

$$D_{ij} = \frac{1}{3} \sum_{k=1}^{n} (\bar{Q}_{ij})_k (h_{k+1}^2 + h_{k+1}h_k + h_k^2) t_k \qquad \text{(A-10)}$$

$$(i, j = 1, 2, 6)$$

where h_k and h_{k+1} are the distances from the reference plane to the upper and lower surfaces, respectively, of the k^{th} lamina, and n is the number of laminae.

The "stability" equations for the laminated curved plate subjected to combined inplane normal and shear loads $\bar{N}_x$, $\bar{N}_y$, and $\bar{N}_{xy}$ are derived here by variational methods (refs. 33 and 34), using the following expressions for the nonlinear "engineering" strains[1] to evaluate the potential energy:

$$\epsilon^{\circ}_x = u_{,x} + \frac{1}{2}\left(v_{,x}{}^2 + w_{,x}{}^2\right) \tag{A-11}$$

$$\epsilon^{\circ}_y = v_{,y} - \frac{w}{R} + \frac{1}{2}u_{,y}{}^2 + \frac{1}{2}\left(w_{,y} + \frac{v}{R}\right)^2 \tag{A-12}$$

$$\gamma^{\circ}_{xy} = u_{,y} + v_{,x} - u_{,x}\,v_{,x} - u_{,y}\left(v_{,y} - \frac{w}{R}\right) + w_{,x}\left(w_{,y} + \frac{v}{R}\right) \tag{A-13}$$

Terms of third or higher degree have been ignored in the above equations. The resulting stability equations are:

$$N_{x,x} + N_{xy,y} - \bar{N}_y\,u_{,yy} - \bar{N}_{xy}\left(\frac{w_{,y}}{R} - v_{,xx} - v_{,yy}\right) = 0 \tag{A-14}$$

$$N_{y,y} + N_{xy,x} - \frac{1}{R}\left(M_{y,y} + 2M_{xy,x}\right) - \bar{N}_x\,v_{,xx} + \frac{\bar{N}_y}{R}\left(w_{,y} + \frac{v}{R}\right) + \bar{N}_{xy}\left(u_{,xx} + u_{,yy} + \frac{w_{,x}}{R}\right) = 0 \tag{A-15}$$

$$M_{x,xx} + M_{y,yy} + 2M_{xy,xy} + \frac{1}{R}N_y - \bar{N}_x\,w_{,xx} - \bar{N}_y\left(w_{,yy} + \frac{v_{,y}}{R}\right) - \bar{N}_{xy}\left(2w_{,xy} + \frac{v_{,x}}{R} - \frac{u_{,y}}{R}\right) = 0 \tag{A-16}$$

The consistent boundary conditions are given below. Along any side y = constant:

$$w = 0 \quad \text{or} \quad \hat{Q} = M_{y,y} + 2M_{xy,x} - \bar{N}_y\left(w_{,y} + \frac{v}{R}\right) - \bar{N}_{xy}\,w_{,x} = 0 \tag{A-17}$$

---

[1]This was communicated to the authors by Dr. Manuel Stein, Structures Division, NASA Langley Research Center, Hampton, Virginia 23365.

$$\theta_y = \left(w_{,y} + \frac{v}{R}\right) = 0 \quad \text{or} \quad \hat{M} = M_y = 0 \tag{A-18}$$

$$v = 0 \quad \text{or} \quad \hat{N} = N_y + \bar{N}_{xy}\, u_{,y} = 0 \tag{A-19}$$

$$u = 0 \quad \text{or} \quad \hat{T} = N_{xy} - \bar{N}_y\, u_{,y} + \bar{N}_{xy}\left(v_{,y} - \frac{w}{R}\right) \tag{A-20}$$

Similarly, along any side x = constant:

$$w = 0 \quad \text{or} \quad \tilde{Q} = M_{x,x} + 2M_{xy,y} - \bar{N}_x\, w_{,x} - \bar{N}_{xy}\left(w_{,y} + \frac{v}{R}\right) = 0 \tag{A-21}$$

$$\theta_x = w_{,x} = 0 \quad \text{or} \quad \tilde{M} = M_x = 0 \tag{A-22}$$

$$v = 0 \quad \text{or} \quad \tilde{T} = N_{xy} - \bar{N}_x\, v_{,x} + \bar{N}_{xy}\, u_{,x} = 0 \tag{A-23}$$

$$u = 0 \quad \text{or} \quad \tilde{N} = N_x + \bar{N}_{xy}\, v_{,x} = 0 \tag{A-24}$$

On substituting equations (A-1), (A-6), and (A-7), the "stability" equations (A-14) to (A-16) may be written as:

$$L_1 u + L_2 v + L_3 w = 0 \tag{A-25}$$

$$L_2 u + L_4 v + L_5 w = 0 \tag{A-26}$$

$$L_3 u + L_5 v + L_6 w = 0 \tag{A-27}$$

The differential operators L_i (i = 1, 2, . . . 6) are commutative and are expressed as:

$$L_1 = A_{11}(\,)_{,xx} + 2A_{16}(\,)_{,xy} + (A_{66} - \bar{N}_y)(\,)_{,yy} \tag{A-28}$$

$$L_2 = \left(A_{16} - \frac{2B_{16}}{R} + \bar{N}_{xy}\right)(\,)_{,xx} + \left(A_{12} + A_{66} - \frac{B_{12}}{R} - \frac{2B_{66}}{R}\right)(\,)_{,xy} + \left(A_{26} - \frac{B_{26}}{R} + \bar{N}_{xy}\right)(\,)_{,yy} \tag{A-29}$$

$$L_3 = -\frac{A_{12}}{R}(\,)_{,x} - \left(\frac{A_{26}}{R} + \frac{\bar{N}_{xy}}{R}\right)(\,)_{,y} - B_{11}(\,)_{,xxx} - (B_{12} + 2B_{66})(\,)_{,xyy} - 3B_{16}(\,)_{,xxy} - B_{26}(\,)_{,yyy} \tag{A-30}$$

$$L_4 = \left(A_{66} - \frac{4B_{66}}{R} + \frac{4D_{66}}{R^2} - N_x\right)(),_{xx} + \left(2A_{26} - \frac{6B_{26}}{R} + \frac{4D_{26}}{R^2}\right)(),_{xy}$$

$$+ \left(A_{22} - \frac{2B_{22}}{R} - \frac{D_{22}}{R^2}\right)(),_{yy} + \frac{\bar{N}_y}{R^2}() \qquad \text{(A-31)}$$

$$L_5 = \left(-\frac{A_{26}}{R} + \frac{2B_{26}}{R^2} + \frac{\bar{N}_{xy}}{R}\right)(),_x + \left(-\frac{A_{22}}{R} + \frac{B_{22}}{R^2} + \frac{\bar{N}_y}{R}\right)(),_y + \left(-B_{16} + \frac{2D_{16}}{R}\right)(),_{xxx}$$

$$+ \left(-B_{12} - 2B_{66} + \frac{D_{12}}{R} + \frac{4D_{66}}{R}\right)(),_{xxy} + \left(-3B_{26} + \frac{4D_{26}}{R}\right)(),_{xyy} \qquad \text{(A-32)}$$

$$+ \left(-B_{22} + \frac{D_{22}}{R}\right)(),_{yyy}$$

$$L_6 = \frac{A_{22}}{R^2}() + \left(\frac{2B_{12}}{R} + \bar{N}_x\right)(),_{xx} + \left(\frac{4B_{26}}{R} + 2\bar{N}_{xy}\right)(),_{xy} + \left(\frac{2B_{22}}{R} + \bar{N}_y\right)(),_{yy}$$

$$+ D_{11}(),_{xxxx} + (2D_{12} + 4D_{66})(),_{xxyy} + 4D_{16}(),_{xxxy} \qquad \text{(A-33)}$$

$$+ 4D_{26}(),_{xyyy} + D_{22}(),_{yyyy}$$

A.2 BUCKLING ANALYSIS

Linear theory is used in the buckling analysis described below. All prebuckling deformations and any initial imperfections are ignored. At buckling, the plate is in a state of uniform external loading. The solution is applicable to (1) finite length plates, when the plate is "specially orthotropic" [i.e., "16" and "26" elements in equations (A-6) and (A-7) are zero] and the combined inplane external loads do not include shear, and (2) infinitely long plates for all other cases. For all plates, arbitrary boundary conditions may be prescribed along the longitudinal sides $y = +\frac{b}{2}$ and $y = -\frac{b}{2}$. For finite length plates, simple support conditions ($w = M_x = v = (N_x + \bar{N}_{xy} \cdot v,_x) = 0$) are stipulated along the sides $x = 0$ and $x = a$.

In the light of the above comments, it is correct to assume buckling displacements that are sinusoidal in the longitudinal (x) direction. A stiffness matrix for a plate strip relating the buckling displacements (w, θ_y, v, u) and the corresponding forces ($\hat{Q}, \hat{M}, \hat{N}, \hat{T}$) along the sides $y = +\frac{b}{2}$ and $y = -\frac{b}{2}$ is derived. These forces and displacements are indicated in figure 26). The elements of the stiffness matrix are transcendental functions of the external loading and half-wavelengths of buckling λ in the x direction. In general, the stiffness matrix is complex and Hermitian in form.

The stiffness matrix is used in formulating the buckling criterion in a determinantal form after enforcing the desired boundary conditions along the sides $y = +\frac{b}{2}$ and $y = -\frac{b}{2}$. For a chosen half-wavelength λ, the buckling load is evaluated by an iteration procedure using the algorithm described in reference 26. A series of half-wavelengths are investigated to determine the minimum buckling load.

The analysis method is such that it can be readily extended to longitudinally stiffened structures subjected to combined inplane normal and shear loads, in a manner analogous to reference 24.

The buckled shape of the laminated plate is defined by the displacement functions:

$$w = \sum_{j=1}^{8} W_j e^{i\alpha_j y} e^{i\beta x} \tag{A-34}$$

$$v = \sum_{j=1}^{8} V_j e^{i\alpha_j y} e^{i\beta x} \tag{A-35}$$

$$u = \sum_{j=1}^{8} U_j e^{i\alpha_j y} e^{i\beta x} \tag{A-36}$$

where $\alpha_j = \frac{p_j y}{a}$, $\beta = \frac{\pi}{\lambda}$ and $i = \sqrt{-1}$.

The p_j are the roots of the characteristic equation obtained by substituting a typical term of the above displacement functions in equations (A-25) to (A-27). This substitution yields:

$$\begin{bmatrix} R_{11} & R_{12} & R_{13} \\ R_{21} & R_{22} & R_{23} \\ R_{31} & R_{32} & R_{33} \end{bmatrix} \begin{Bmatrix} U_j \\ V_j \\ W_j \end{Bmatrix} = 0 \tag{A-37}$$

The characteristic equation mentioned earlier is obtained by expanding the determinant of the matrix [R]. This equation is an eighth order polynomial in p_j (or α_j) with real coefficients and hence has real or complex conjugate roots.

Also from equation (A-37), U_j and V_j can be readily expressed in terms of W_j as:

$$U_j = \bar{L}_{2j} W_j \tag{A-38}$$

$$V_j = \bar{L}_{1j} W_j \tag{A-39}$$

It is evident that the roots p_j (or α_j) are functions of the external loading ($\bar{N}_x$, $\bar{N}_y$, and $\bar{N}_{xy}$) and the half-wavelength of buckling λ. At selected values of these quantities, using appropriate values of y ($+\frac{b}{2}$ or $-\frac{b}{2}$), the buckling displacements defined by w, θ_y, v, and u along the sides of a plate strip are evaluated from:

$$w = \sum_{j=1}^{8} e^{i\alpha_j y} W_j e^{i\beta x} \tag{A-40}$$

$$\theta_y = w_{,y} + \frac{v}{R} = \sum_{j=1}^{8} (i\alpha_j + \frac{1}{R} \bar{L}_{1j}) e^{i\alpha_j y} W_j e^{i\beta x} \tag{A-41}$$

$$v = \sum_{j=1}^{8} \bar{L}_{1j} e^{i\alpha_j y} W_j e^{i\beta x} \tag{A-42}$$

$$u = \sum_{j=1}^{8} \bar{L}_{2j} e^{i\alpha_j y} W_j e^{i\beta x} \tag{A-43}$$

Defining the vector $\{d\}$ as

$$\{d\} = \{w, \theta_y, v, u\}^T \tag{A-44}$$

displacements from equations (A-40) and (A-41) may be written in matrix form as:

$$\begin{Bmatrix} d^- \\ d^+ \end{Bmatrix} = \begin{bmatrix} X_d^- \\ X_d^+ \end{bmatrix} \{r\} \tag{A-45}$$

where $\{r\} = \{W_1 e^{i\beta x}, W_2 e^{i\beta x}, \ldots W_8 e^{i\beta x}\}^T$ and $[X_d]$ is a 4 x 8 submatrix. The superscripts - and + are used to denote the sides of the plate strip corresponding to $y = -\frac{b}{2}$ and $y = +\frac{b}{2}$, respectively.

The forces corresponding to the above buckling displacements are, from equations (A-17) to (A-20):

$$\hat{Q} = \sum_{j=1}^{8} \Big\{ -B_{12}\alpha_j \beta \bar{L}_{2j} - B_{22}\alpha_j (\bar{L}_{1j}\alpha_j + \frac{i}{R}) - B_{26} (\bar{L}_{2j}\alpha_j^2 + 3\,\bar{L}_{1j}\alpha_j \beta + \frac{2i\beta}{R})$$

$$+ i\,D_{12}\alpha_j\beta^2 + D_{22}\alpha_j^2 (i\alpha_j + \frac{1}{R}\,\bar{L}_{1j}) + 4\,D_{66}\alpha_j\beta (i\alpha_j + \frac{1}{R}\,\bar{L}_{1j})$$

$$-2\,B_{16}\,\bar{L}_{2j}\beta^2 - 2\,B_{66}\beta (\bar{L}_{2j}\alpha_j + \bar{L}_{1j}\beta)$$

$$+2\,D_{16}\,i\beta^3 + 4\,D_{66}\beta^2 (i\alpha_j + \frac{1}{R}\bar{L}_{1j})$$

$$-\bar{N}_y (\frac{1}{R}\bar{L}_{1j} + i\alpha_j) - \bar{N}_{xy}\,i\beta \Big\} e^{i\alpha_j y} W_j e^{i\beta x} \qquad \text{(A-46)}$$

$$\hat{M} = \sum_{j=1}^{8} \Big\{ B_{12}\,\bar{L}_{2j}\,i\beta + B_{22} (\bar{L}_{1j}\,i\alpha_j - \frac{1}{R}) + i\,B_{26} (\bar{L}_{2j}\alpha_j + \bar{L}_{1j}\beta)$$

$$+ D_{12}\beta^2 + D_{22}\alpha_j (\alpha_j - \frac{1}{R}\bar{L}_{1j}\,i)$$

$$+ 2\,D_{66}\beta (\alpha_j - \frac{1}{R}\bar{L}_{1j}\,i) \Big\} e^{i\alpha_j y} W_j e^{i\beta x} \qquad \text{(A-47)}$$

$$\hat{N} = \sum_{j=1}^{8} \Big\{ A_{12}\,\bar{L}_{2j}\,i\beta + A_{22} (\bar{L}_{1j}\,i\alpha_j - \frac{1}{R}) + A_{26}\,i (\bar{L}_{2j}\alpha_j + \bar{L}_{1j}\beta)$$

$$+B_{12}\beta^2 + B_{22}\alpha_j (\alpha_j - \frac{1}{R}\,\bar{L}_{1j}\,i)$$

$$+2\,B_{26}\beta (\alpha_j - \frac{1}{R}\,\bar{L}_{1j}\,i) + \bar{N}_{xy}\,\bar{L}_{2j}\,i\alpha_j \Big\} e^{i\alpha_j y} W_j e^{i\beta x} \qquad \text{(A-48)}$$

$$\hat{T} = \sum_{j=1}^{8} \Big\{ A_{16}\,\bar{L}_{2j}\,i\beta + A_{26} (\bar{L}_{1j}\alpha_j i - \frac{1}{R}) + A_{66} (\bar{L}_{2j}\alpha_j i + \bar{L}_{1j}\beta\,i)$$

$$+B_{16}\beta^2 + B_{26}\,\alpha_j (\alpha_j - \frac{1}{R}\bar{L}_{1j}\,i) + 2\,B_{66}\beta (\alpha_j - \frac{1}{R}\bar{L}_{1j}\,i)$$

$$-\bar{N}_y\,\bar{L}_{2j}\alpha_j\,i + \bar{N}_{xy} (\bar{L}_{1j}\alpha_j\,i - \frac{1}{R}) \Big\} e^{i\alpha_j y} W_j e^{i\beta x} \qquad \text{(A-49)}$$

Again defining a vector $\{f\}$ as

$$\{f\} = \{\hat{Q}, \hat{M}, \hat{N}, \hat{T}\}^T \tag{A-50}$$

the forces corresponding to the buckling displacements in equation (A-45) may be written in matrix form as:

$$\begin{Bmatrix} f^- \\ f^+ \end{Bmatrix} = \begin{bmatrix} X_f^- \\ \hline X_f^+ \end{bmatrix} \begin{Bmatrix} r \end{Bmatrix} \tag{A-51}$$

where $[X_f]$ is a 4 x 8 submatrix.

Equations (A-45) and (A-51) are combined to yield:

$$\begin{Bmatrix} f^- \\ f^+ \end{Bmatrix} = \begin{bmatrix} X_f^- \\ \hline X_f^+ \end{bmatrix} \begin{bmatrix} X_d^- \\ \hline X_d^+ \end{bmatrix}^{-1} \begin{Bmatrix} d^- \\ d^+ \end{Bmatrix} \tag{A-52}$$

or

$$\begin{Bmatrix} f^- \\ f^+ \end{Bmatrix} = \begin{bmatrix} s \end{bmatrix} \begin{Bmatrix} d^- \\ d^+ \end{Bmatrix} \tag{A-53}$$

[s] in the above equation is the stiffness matrix (8 x 8) of the laminated curved plate and defines the force-displacement (due to buckling) relationship along the two sides $y = -\frac{b}{2}$ and $y = +\frac{b}{2}$. The stiffness matrix is in general complex and Hermitian in form.

Equation (A-53) is used in formulating the buckling criterion after enforcing the desired boundary conditions along the above-mentioned sides. The boundary conditions are stipulated by specified restraints to freedoms in the directions of w, θ_y, v, and u displacements along each side. It is evident that, if a displacement is chosen to be unrestrained, the stiffness matrix remains unaltered since the corresponding force is zero. Similarly, if complete restraint to a chosen displacement is desired, the corresponding row and column of the stiffness matrix may be deleted, as is often done in discrete (finite) element method of structural analysis.

Since plate buckling is primarily an out-of-plane phenomenon, the components w and θ_y of the displacement vector and the corresponding stiffness terms in equation (A-53) are of utmost significance. Hence, difficulties could arise in cases where these degrees of freedom are completely restrained along both sides of the plate, and the corresponding rows and columns of the stiffness

matrix are deleted. In the buckling formulation used here, the "full plate" is considered as an assembly of two "half-plates" joined along the longitudinal midline. Thus, all the four degrees of freedom (w, θ_y, v, and u) are always retained along this line, thereby avoiding the above-mentioned difficulty. Finally, if any of the boundary conditions stipulated along the two sides are arbitrary and specified by spring constants (k_w, k_θ, k_v, or k_u), the latter may be readily added to the corresponding diagonal elements of the stiffness matrix in equation (A-53).

The buckling formulation may be summarized to consist of the following steps:

1) Evaluate the stiffness matrix (8 x 8) as in equation (A-53) for one half-plate. The stiffness matrix for the other half-plate is identical.

2) Form the merged stiffness matrix (12 x 12) for a full plate.

3) Enforce the specified boundary conditions along the two sides of the plate by modifying the merged stiffness matrix, as discussed earlier.

The above procedure results in the equation:

$$[S] \{\delta\} = 0 \qquad \text{(A-54)}$$

where $\{\delta\}$ is the vector of buckling displacements corresponding to the modified merged stiffness matrix [S]. A nontrivial solution of the above equation is expressed in the determinantal form:

$$|S| = 0 \qquad \text{(A-55)}$$

The elements of [S] are transcendental functions of the applied loads ($\bar{N}_x$, $\bar{N}_y$, and $\bar{N}_{xy}$) and the half-wavelength of buckling λ in the x direction. The lowest level of the applied loads at which equation (A-55) is satisfied is the buckling load of the laminated plate for a chosen λ. This load is determined using an iteration algorithm discussed in reference 26 and further illustrated in reference 24. The algorithm requires an upper bound to the buckling load defined as the buckling load of the half-plate when both of its longitudinal sides are completely restrained. Such an upper bound load may be readily obtained using the Galerkin method (ref. 35), in the manner of reference 24.

A series of half-wavelengths have to be investigated, and the lowest of all the corresponding buckling loads is the critical load for the laminated plate. The strains in the plate at the critical load are obtained from equations (A-6) and (A-7) as:

$$\begin{Bmatrix} \epsilon_x \\ \epsilon_y \\ \gamma_{xy} \end{Bmatrix} = [A^*]^{-1} \begin{Bmatrix} \bar{N}_x \\ \bar{N}_y \\ \bar{N}_{xy} \end{Bmatrix} \tag{A-56}$$

where $A^* = A - B D^{-1} B$

The above strains are with respect to the x, y coordinates. For fiber-reinforced composite plates, appropriate coordinate transformation yields the fiber strain at the critical load.

For flat plates, certain simplifications in the numerical solution, similar to that described in reference 24, are possible when the elements of the B matrix in equations (A-6) and (A-7) are identically zero.

APPENDIX B

CONVERSION OF U. S. CUSTOMARY UNITS TO SI UNITS

The International System of Units (SI) was adopted by the Eleventh General Conference on Weights and Measures, Paris, October 1960, in Resolution No. 12. (See ref. 36). Conversion factors for the units used herein are given in the following tables:

Physical quantity	U.S. customary unit	Conversion factor (*)	SI unit (**)
Area	$in.^2$	6.452×10^{-4}	square meters (m^2)
Force	kip = 1000 lbf	4.448×10^{3}	newtons (N)
Length	in.	2.54×10^{-2}	meters (m)
Moduli and stress	ksi = 1000 $lbf/in.^2$	6.895×10^{6}	newtons per square meter (N/m^2)
Stress resultant	lbf/in.	175.1	newtons per meter (N/m)
Density	$lbm/in.^3$	27.68×10^{3}	kilograms per cubic meter (kg/m^3)

*Multiple value given in U.S. customary unit by conversion factor to obtain equivalent value in SI unit.

**Prefixes to indicate multiple of units are as follows:

Prefix	Multiple
milli (m)	10^{-3}
centi (c)	10^{-2}
kilo (k)	10^{3}
giga (G)	10^{9}

TABLE 1.–MATERIAL PROPERTIES

No	Material	V_f	$E_{11} \times 10^{-10}$ N/m^2	$E_{22} \times 10^{-10}$ N/m^2	ν_{12}	$G_{12} \times 10^{-10}$ N/m^2	ρ, kg/m^3
1.	Boron/epoxy	0.5	20.69	1.86	0.21	0.48	2006.8
2.	Boron/aluminum	0.5	20.69	13.1	0.23	6.55	2712.6
3.	High modulus graphite/epoxy	0.6	17.24	1.17	0.3	0.45	1605.4
4.	Borsic/aluminum	0.5	20.69	13.1	0.26	4.69	2712.6
5.	Aluminum 2024		7.38	7.38	0.33	2.76	2768.0

TABLE 2.–BUCKLING RESULTS FOR CURVED LAMINATE A. LOADING: $\bar{N}_x$

$\frac{b^2}{R\tilde{t}}$	Buckling loads, N/m, and $\frac{\lambda}{b}$ ratios							
	BC-uv	$\frac{\lambda}{b}$	BC-vN_{xy}	$\frac{\lambda}{b}$	BC-uN_y	$\frac{\lambda}{b}$	BC-$N_y N_{xy}$	$\frac{\lambda}{b}$
1	9 788	0.75	9 788	0.75	9 753	0.75	9 736	0.75
5	11 434	0.69	11 346	0.69	10 681	0.74	10 331	0.76
10	15 426	0.58	15 200	0.59	13 518	0.7	12 117	0.77
30	36 578	0.38	36 263	0.38	34 705	0.42	28 191	1.22
50	56 750	0.32	56 365	0.33	52 365	0.39	46 892	0.5
100	101 540	0.26	101 190	0.26	97 145	0.30	90 422	0.8
300	241 585	0.19	241 375	0.19	237 891	0.20	191 524	4.8
500	324 986	0.16	324 898	0.16	322 044	0.17	172 754	7.2
700	366 870	0.14	366 764	0.15	253 842	15.6	112 222	10.4
1000	386 498	0.13	386 428	0.13	61 810	36.7	27 053	24.5

TABLE 3.–BUCKLING RESULTS FOR CURVED LAMINATE A.[a]
LOADING: $\bar{N}_y$

$\frac{b^2}{R\tilde{t}}$	Buckling loads, N/m			
	BC-uv	BC-vN_{xy}	BC-uN_y	BC-$N_y N_{xy}$
1	5 813	5 813	5726	1191
5	8 020	7 792	5726	1366
10	11 697	11 697	5726	1401
30	11 697	11 697	5708	1418
50	11 662	11 662	5691	1418
100	11 557	11 557	5638	1401
300	10 541	10 541	3852	1261
500	9 088	9 070	2224	1051
700	7 652	7 634	1593	858
1000	5 866	5 831	1121	648

[a]All buckling loads are at limiting $\frac{\lambda}{b}$ value of 250.

TABLE 4.–BUCKLING RESULTS FOR CURVED LAMINATE A. LOADING: $\bar{N}_{xy}$

$\frac{b^2}{Rt}$	Buckling loads, N/m, and $\frac{\lambda}{b}$ ratios											
	BC-uv	$\frac{\lambda}{b}$	BC-vN_{xy}	$\frac{\lambda}{b}$	BC-uN_y	$\frac{\lambda}{b}$	BC-$N_y N_{xy}$	$\frac{\lambda}{b}$	BC-uN_{v_y}	$\frac{\lambda}{b}$	BC-$N_{xy_v} N_y$	$\frac{\lambda}{b}$
1	12 415	0.85	12 415	0.85	12 380	0.85	12 380	0.85	12 397	0.85	12 397	0.85
5	13 413	0.80	13 360	0.80	12 870	0.85	12 660	0.86	13 130	0.83	12 960	0.84
10	15 580	0.72	15 440	0.73	14 220	0.85	13 450	0.89	14 950	0.77	14 500	0.82
30	24 200	0.58	24 000	0.59	21 780	0.75	18 630	1.20	23 040	0.65	22 120	0.71
50	31 170	0.59	30 960	0.60	27 930	0.75	23 460	1.59	29 560	0.67	28 230	0.74
100	44 840	0.62	44 580	0.63	39 430	0.94	32 530	2.33	42 430	0.74	39 940	0.93
300	74 120	0.86	72 950	0.95	64 170	1.22	41 360	22.8	69 230	1.05	64 840	1.19
500	82 860	1.03	81 020	1.18	70 670	2.15	23 450	26.7	77 360	1.14	71 950	1.51
700	82 630	1.02	80 280	1.31	70 970	2.43	12 920	19.5	76 610	1.52	71 530	1.65
1000	75 630	1.32	73 510	1.45	25 140	75.0	3 992	27.7	70 530	1.71	65 910	1.87

TABLE 5.–BUCKLING RESULTS FOR CURVED LAMINATE A
LOADING: $\bar{N}_x = \bar{N}_{xy}$

$\frac{b^2}{R\tilde{t}}$	Buckling loads, N/m, and $\frac{\lambda}{b}$ ratios											
	BC-uv	$\frac{\lambda}{b}$	BC-vN_{xy}	$\frac{\lambda}{b}$	BC-uN_y	$\frac{\lambda}{b}$	BC-$N_y N_{xy}$	$\frac{\lambda}{b}$	BC-u$N_v y$	$\frac{\lambda}{b}$	BC-$N_{xy} N_v y$	$\frac{\lambda}{b}$
1	6 951	0.78	6 951	0.78	6 934	0.78	6 934	0.78	6 951	0.78	6 934	0.78
5	7 792	0.72	7 739	0.73	7 389	0.78	7 214	0.79	7 582	0.75	7 459	0.77
10	9 666	0.6	9 560	0.61	8 650	0.75	8 002	0.82	9 175	0.69	8 825	0.72
30	16 897	0.51	16 757	0.51	15 426	0.6	13 273	1.15	16 179	0.55	15 496	0.60
50	22 921	0.48	22 781	0.49	20 872	0.6	18 105	1.58	21 923	0.54	20 959	0.60
100	35 143	0.48	34 967	0.49	31 938	0.72	27 000	2.36	33 654	0.55	32 096	0.67
300	63 526	0.67	62 931	0.72	56 190	1.54	37 962	22.8	60 077	0.88	56 330	1.07
500	73 104	0.86	71 914	0.93	63 947	1.40	22 308	19.3	68 692	1.14	63 947	1.35
700	73 770	0.99	72 439	0.96	64 209	1.57	12 327	19.1	69 445	1.11	64 227	1.56
1000	68 587	1.17	66 836	1.28	22 290	56.0	3 712	27.3	64 297	1.48	59 727	1.81

TABLE 6.–BUCKLING RESULTS FOR CURVED LAMINATE A.
LOADING: $N_y = N_{xy}$

$\frac{b^2}{R\tilde{t}}$	Buckling loads, N/m, and $\frac{\lambda}{b}$ ratios											
	BC-uv	$\frac{\lambda}{b}$	BC-vN_{xy}	$\frac{\lambda}{b}$	BC-uN_y	$\frac{\lambda}{b}$	BC-$N_y N_{xy}$	$\frac{\lambda}{b}$	BC-uN_y	$\frac{\lambda}{b}$	BC-$N_{xy_v} N_y$	$\frac{\lambda}{b}$
1	5 516	2.07	5 480	1.66	5430	1.7	1190	[a]250	5550	3.06	5533	2.98
5	6 566	1.22	6 496	1.25	5550	2.74	1366	[a]250	5726	6.51	5570	2.37
10	8 160	1.0	8·040	1.0	5640	3.47	1420	[a]250	5726	[a]250	5656	4.38
30	11 400	1.7	11 120	1.8	5708	10.1	1420	[a]250	5708	[a]250	5708	14.5
50	11 660	[a]250	11 520	4.6	5690	[a]250	1420	[a]250	5690	[a]250	5690	23.4
100	11 560	[a]250	11 520	8.7	5620	33.4	1400	[a]250	5620	[a]250	5620	40.0
300	10 540	[a]250	10 520	28.2	3850	25.0	1260	[a]250	4950	[a]250	4830	[a]250
500	9 090	[a]250	9 070	125	2220	[a]250	1050	[a]250	3570	[a]250	3200	[a]250
700	7 650	[a]250	7 630	[a]250	1590	[a]250	860	65	2100	[a]250	1580	[a]250
1000	5 880	[a]250	5 830	[a]250	1120	[a]250	650	65	1140	[a]250	665	[a]250

[a]Limiting value allowed

TABLE 7.–BUCKLING RESULTS FOR CURVED LAMINATE A. LOADING: $\bar{N}_x = \bar{N}_y$

$\frac{b^2}{R\tilde{t}}$	Buckling loads, N/m, and $\frac{\lambda}{b}$ ratios							
	BC-uv	$\frac{\lambda}{b}$	BC-vN_{xy}	$\frac{\lambda}{b}$	BC-uN_y	$\frac{\lambda}{b}$	BC-$N_y N_{xy}$	$\frac{\lambda}{b}$
1	4 868	1.2	4 868	1.2	4833	1.2	648	[a]250
5	6 251	1.0	6 164	1.0	5130	1.4	1138	[a]250
10	9 508	0.8	9 263	0.8	5516	2.8	1331	239
30	11 697	[a]250	11 662	5.3	5691	8.0	1418	[a]250
50	11 662	[a]250	11 662	11.1	5691	12.5	1418	[a]250
100	11 557	[a]250	11 557	16.7	5621	50	1401	[a]250
300	10 541	[a]250	10 541	46.7	3852	[a]250	1261	[a]250
500	9 088	[a]250	9 070	[a]250	2224	[a]250	1051	[a]250
700	7 652	[a]250	7 634	[a]250	1593	[a]250	858	[a]250
1000	5 866	[a]250	5 831	[a]250	1121	[a]250	648	[a]250

[a]Limiting value allowed

TABLE 8.–BUCKLING RESULTS FOR CURVED LAMINATE A.
LOADING: $\bar{N}_x = \bar{N}_y = \bar{N}_{xy}$

$\frac{b^2}{R\tilde{t}}$	Buckling loads, N/m, and $\frac{\lambda}{b}$ ratios											
	BC-uv	$\frac{\lambda}{b}$	BC-vN_{xy}	$\frac{\lambda}{b}$	BC-uN_y	$\frac{\lambda}{b}$	BC-$N_y N_{xy}$	$\frac{\lambda}{b}$	BC-uN_{y_y}	$\frac{\lambda}{b}$	BC-$N_{xy_y} N_y$	$\frac{\lambda}{b}$
1	4 290	1.1	4 290	1.1	4250	1.1	650	[a]250	4290	1.2	4270	1.2
5	5 110	0.9	5 060	0.9	4520	1.2	1140	[a]250	4830	1.3	4610	1.3
10	6 600	0.79	6 515	0.8	5060	1.6	1330	229	5725	[a]250	5270	2.1
30	10 560	0.92	10 470	1.0	5670	11.3	1420	229	5710	[a]250	5660	10.3
50	11 660	[a]250	11 350	3.2	5660	9.7	1420	[a]250	5690	[a]250	5670	12.6
100	11 560	[a]250	11 490	7.0	5620	19.8	1400	[a]250	5620	[a]250	5620	29.5
300	10 540	[a]250	10 520	20.5	3850	[a]250	1260	[a]250	4955	[a]250	4830	67
500	9 090	[a]250	9 070	37	2150	[a]250	1050	[a]250	3570	[a]250	3200	114
700	7 650	[a]250	7 630	[a]250	1590	[a]250	860	[a]250	2100	[a]250	1575	153
1000	5 880	[a]250	5 830	[a]250	1120	[a]250	650	63.5	1140	[a]250	665	[a]250

[a]Limiting value allowed

TABLE 9.—BUCKLING RESULTS FOR CURVED LAMINATE B (ODD NUMBER OF LAYERS)

	Number of layers							
	1	3	5	7	9	11	13	15
Present analysis								
λ/b	10.0	6.2	4.9	4.1	3.7	3.3	3.2	2.9
$\bar{N}_x$, N/m	452	4553	13 518	28 016	48 695	76 221	111 224	154 298
16, 26 = 0								
λ/b	10.6	6.2	4.8	4.1	3.7	3.4	3.2	2.9
$\bar{N}_x$, N/m	499	4745	13 850	28 489	49 291	76 921	112 064	155 279
Present analysis								
λ/b	[a]250	[a]250	[a]250	[a]250	[a]250	[a]250	[a]250	[a]250
$\bar{N}_y$, N/m	2	53	280	753	1593	2907	4798	7372
16, 26 = 0								
λ/b	[a]250	[a]250	[a]250	[a]250	[a]250	[a]250	[a]250	[a]250
$\bar{N}_y$, N/m	2	53	280	753	1593	2907	4798	7372
Present analysis								
λ/b	9.9	6.2	4.8	4.2	3.8	3.5	3.2	3.0
$\bar{N}_{xy}$, N/m	88	1471	5253	12 345	23 498	39 538	61 390	89 301
16, 26 = 0								
λ/b	9.4	6.1	4.8	4.1	3.7	3.4	3.2	2.9
$\bar{N}_{xy}$, N/m	77	1243	4588	10 979	21 240	36 123	56 400	82 857
Present analysis								
λ/b	9.9	6.1	4.8	4.1	3.7	3.4	3.2	3.0
$\bar{N}_x = \bar{N}_{xy}$, N/m	70	1278	4413	10 068	18 736	30 940	47 119	67 746
16, 26 = 0								
λ/b	10.3	6.1	4.8	4.1	3.7	3.4	3.2	3.0
$\bar{N}_x = \bar{N}_{xy}$, N/m	70	1086	3870	9018	17 037	28 419	43 652	63 176

[a]Limiting value allowed

TABLE 10.—BUCKLING RESULTS FOR CURVED LAMINATE B (EVEN NUMBER OF LAYERS)

	Number of layers						
	2	4	6	8	10	12	14
Present analysis							
λ/b	8.8	5.5	4.5	3.9	3.5	3.3	3.1
$\bar{N}_x$, N/m	1453	8055	19 786	37 366	61 460	92 698	131 745
16, 26 = 0							
λ/b	7.5	5.4	4.5	3.9	3.5	3.2	3.0
$\bar{N}_x$, N/m	2049	8650	20 434	38 084	62 213	93 521	132 620
RBS							
λ/b	8.8	5.5	4.6	3.9	3.5	3.3	3.1
$\bar{N}_x$, N/m	1453	8055	19 786	37 366	61 460	92 698	131 745
Present analysis							
λ/b	[a]250	[a]250	[a]250	[a]250	[a]250	[a]250	[a]250
$\bar{N}_y$, N/m	9	123	455	1086	2136	3712	5936
16, 26 = 0							
λ/b	[a]250	[a]250	[a]250	[a]250	[a]250	[a]250	[a]250
$\bar{N}_y$, N/m	18	140	473	1121	2189	3765	5988
RBS							
λ/b	[a]250	[a]250	[a]250	[a]250	[a]250	[a]250	[a]250
$\bar{N}_y$, N/m	9	123	455	1086	2136	3730	5936
Present analysis							
λ/b	8.5	5.3	4.4	3.9	3.5	3.3	3.1
$\bar{N}_{xy}$, N/m	263	2294	6951	15 059	27 386	44 721	67 816
16, 26 = 0							
λ/b	7.4	5.4	4.5	3.9	3.6	3.3	3.1
$\bar{N}_{xy}$, N/m	438	2574	7354	15 584	28 051	45 544	68 814
RBS							
λ/b	8.6	5.4	4.5	3.9	3.6	3.3	3.1
$\bar{N}_{xy}$, N/m	263	2329	7039	15 200	27 596	45 018	68 219
Present analysis							
λ/b	8.4	5.4	4.4	3.9	3.5	3.2	3.1
$\bar{N}_x = \bar{N}_{xy}$, N/m	228	1979	5796	12 204	21 747	34 880	52 092
16, 26 = 0							
λ/b	7.4	5.3	4.4	3.9	3.5	3.3	3.1
$\bar{N}_x = \bar{N}_{xy}$, N/m	403	2206	6111	12 625	22 273	35 528	52 845
RBS							
λ/b	8.7	5.5	4.4	3.9	3.5	3.3	3.1
$\bar{N}_x = \bar{N}_{xy}$, N/m	245	2014	5848	12 327	21 940	35 143	52 425

[a]Limiting value allowed

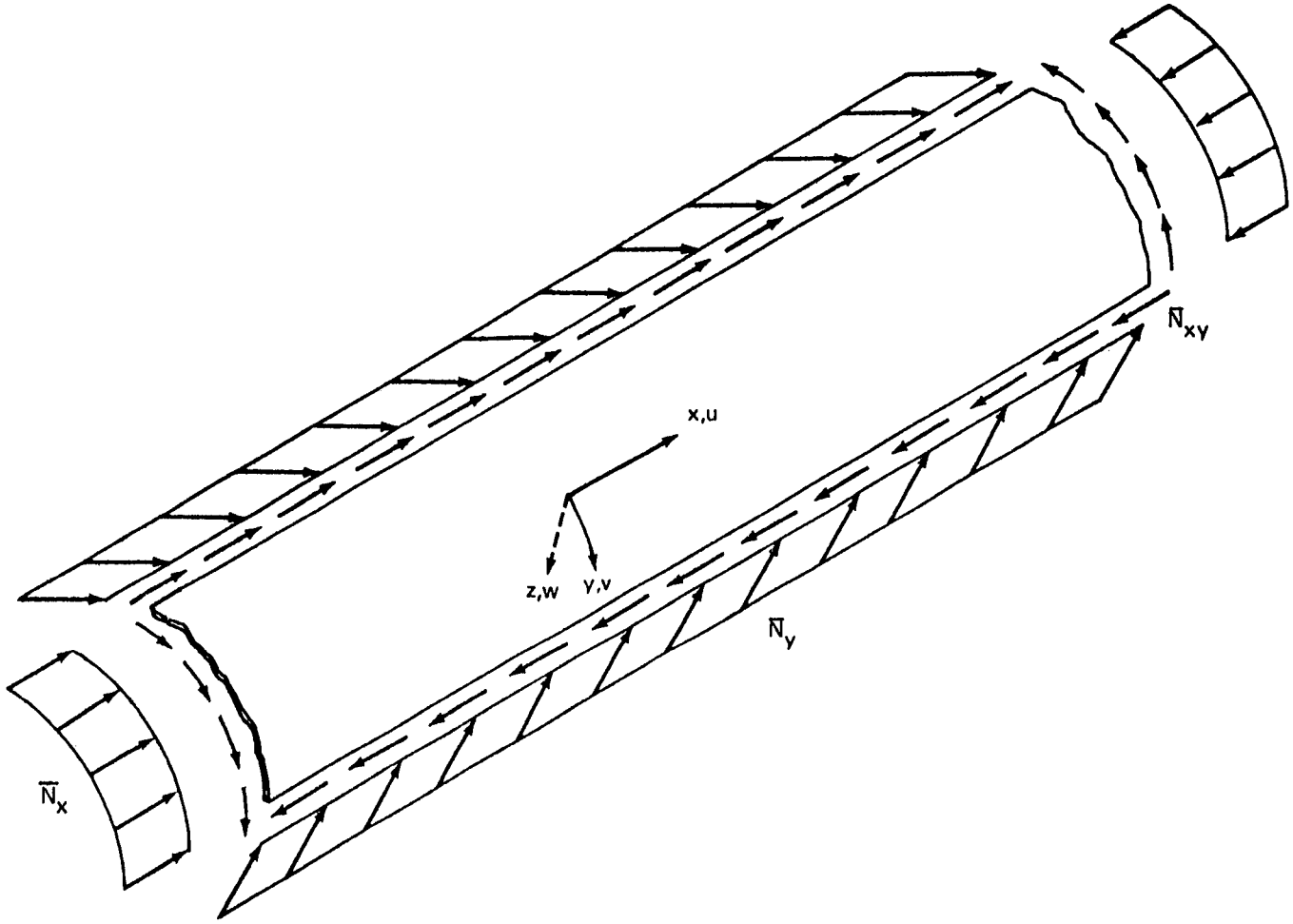

FIGURE 1.—LONG CURVED PLATE SUBJECTED TO COMBINED INPLANE LOADS

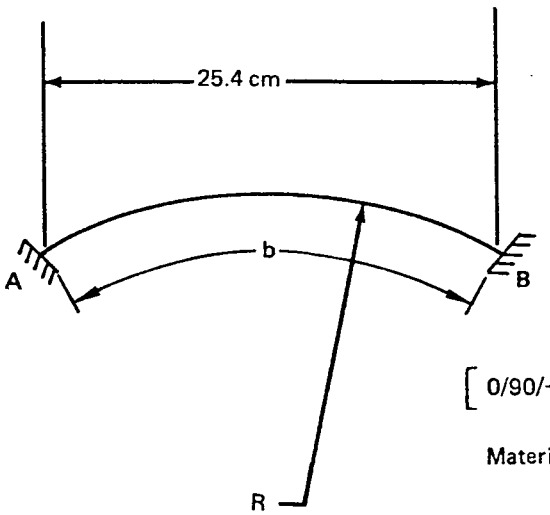

$\left[0/90/+45/-45 \right]_s$

Material: boron/epoxy

Thickness of each lamina: 0.014 cm

Total thickness $\tilde{t}$ = 0.112 cm

Boundary condition code	Inplane boundary conditions on clamped edge A	Inplane boundary conditions on clamped edge B
uv	$u = v = 0$	$u = v = 0$
vN_{xy}	$v = N_{xy} = 0$	$v = N_{xy} = 0$
uN_y	$u = N_y = 0$	$u = N_y = 0$
N_yN_{xy}	$N_y = N_{xy} = 0$	$N_y = N_{xy} = 0$
uN_y (v)	$u = N_y = 0$	$u = v = 0$
$N_{xy}N_y$ (v)	$N_{xy} = N_y = 0$	$N_{xy} = v = 0$

FIGURE 2.—GEOMETRY AND INPLANE BOUNDARY CONDITIONS FOR CURVED LAMINATE A

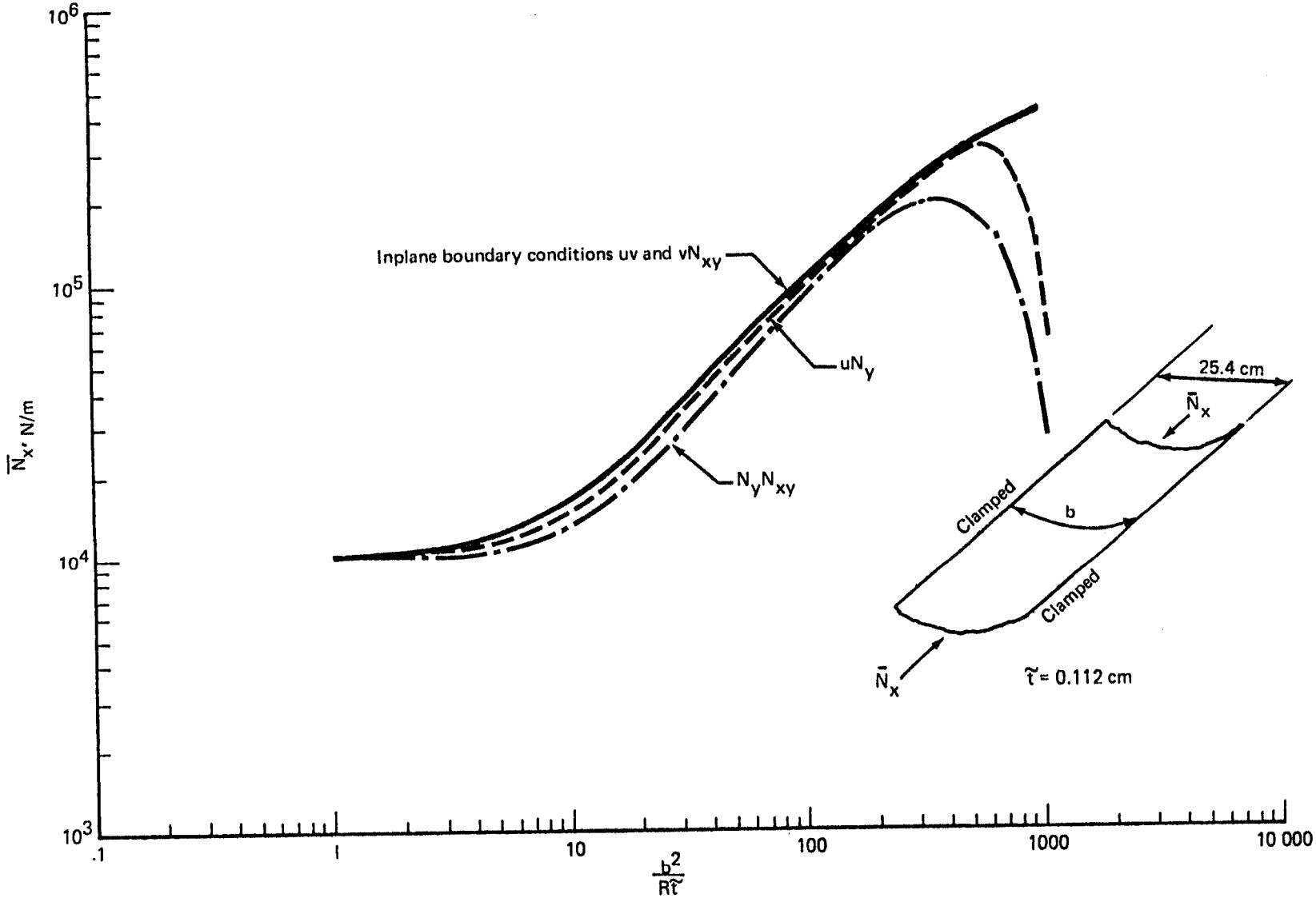

FIGURE 3.–BUCKLING RESULTS FOR CURVED LAMINATE A LOADING: $\bar{N}_x$

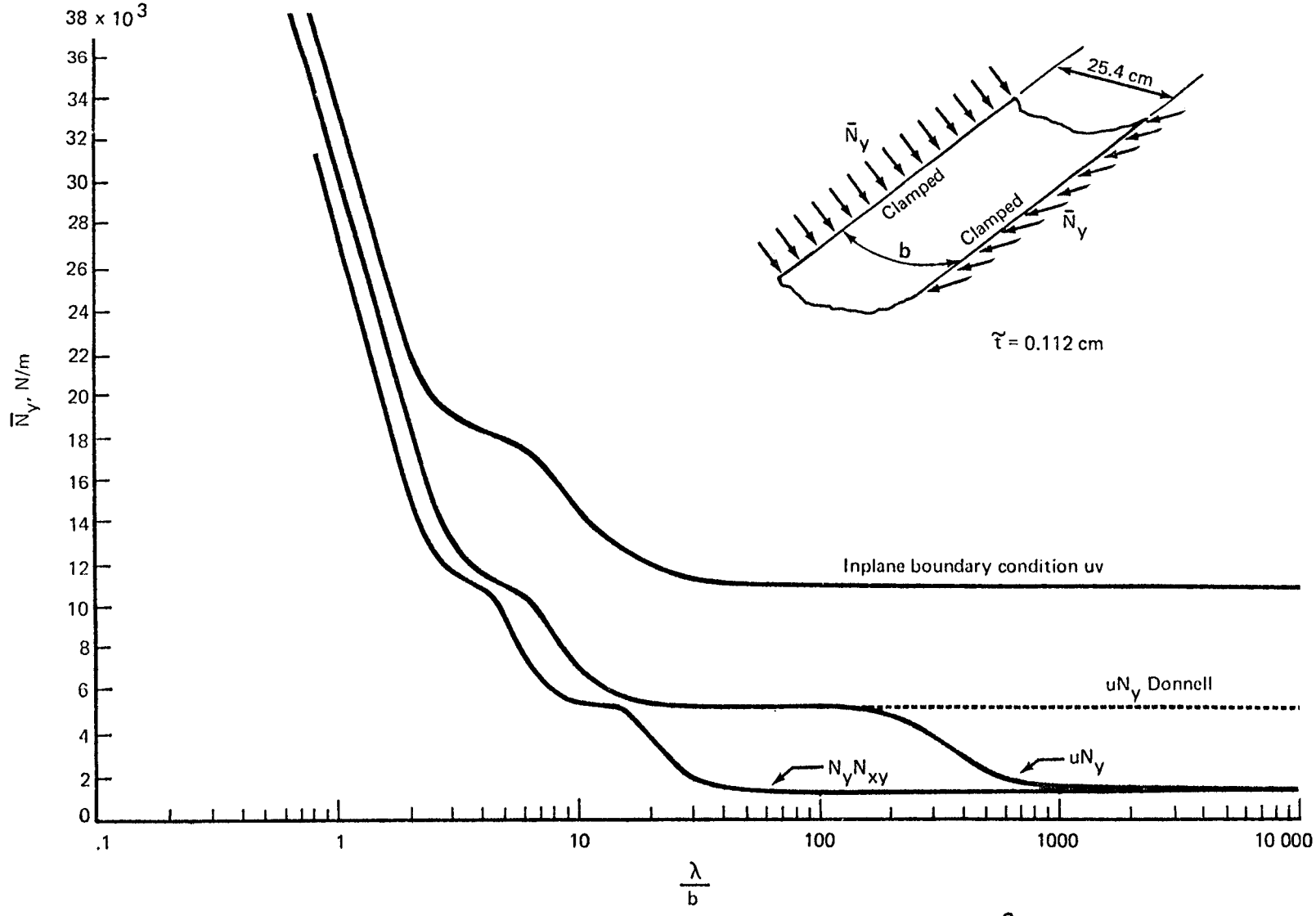

FIGURE 4.–BUCKLING RESULTS FOR CURVED LAMINATE A $\left(\frac{b^2}{R\tilde{t}} = 300\right)$
LOADING: $\bar{N}_y$

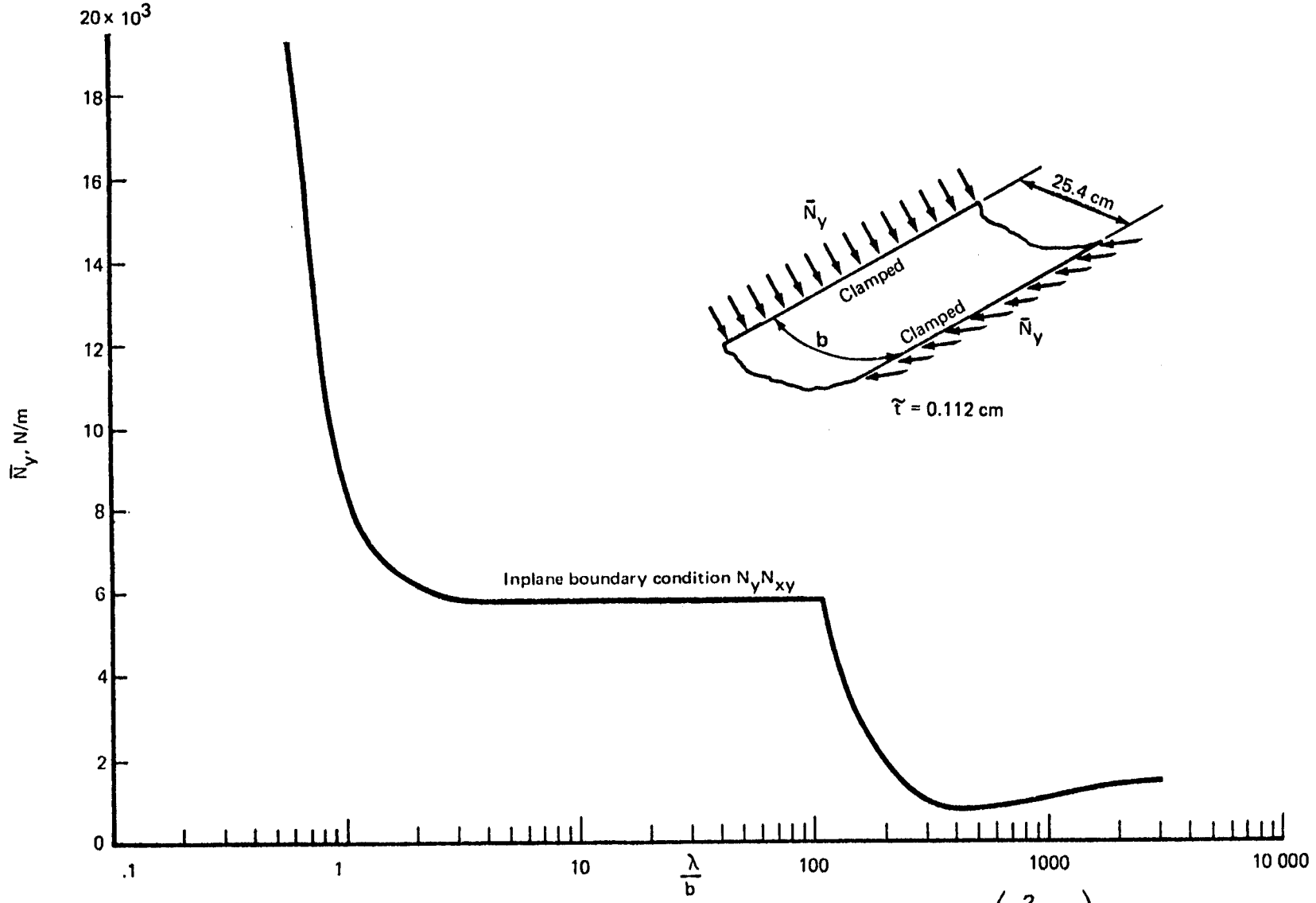

FIGURE 5.–BUCKLING RESULTS FOR CURVED LAMINATE A $\left(\frac{b^2}{R\tilde{t}} = 1.0\right)$
LOADING: $\bar{N}_y$

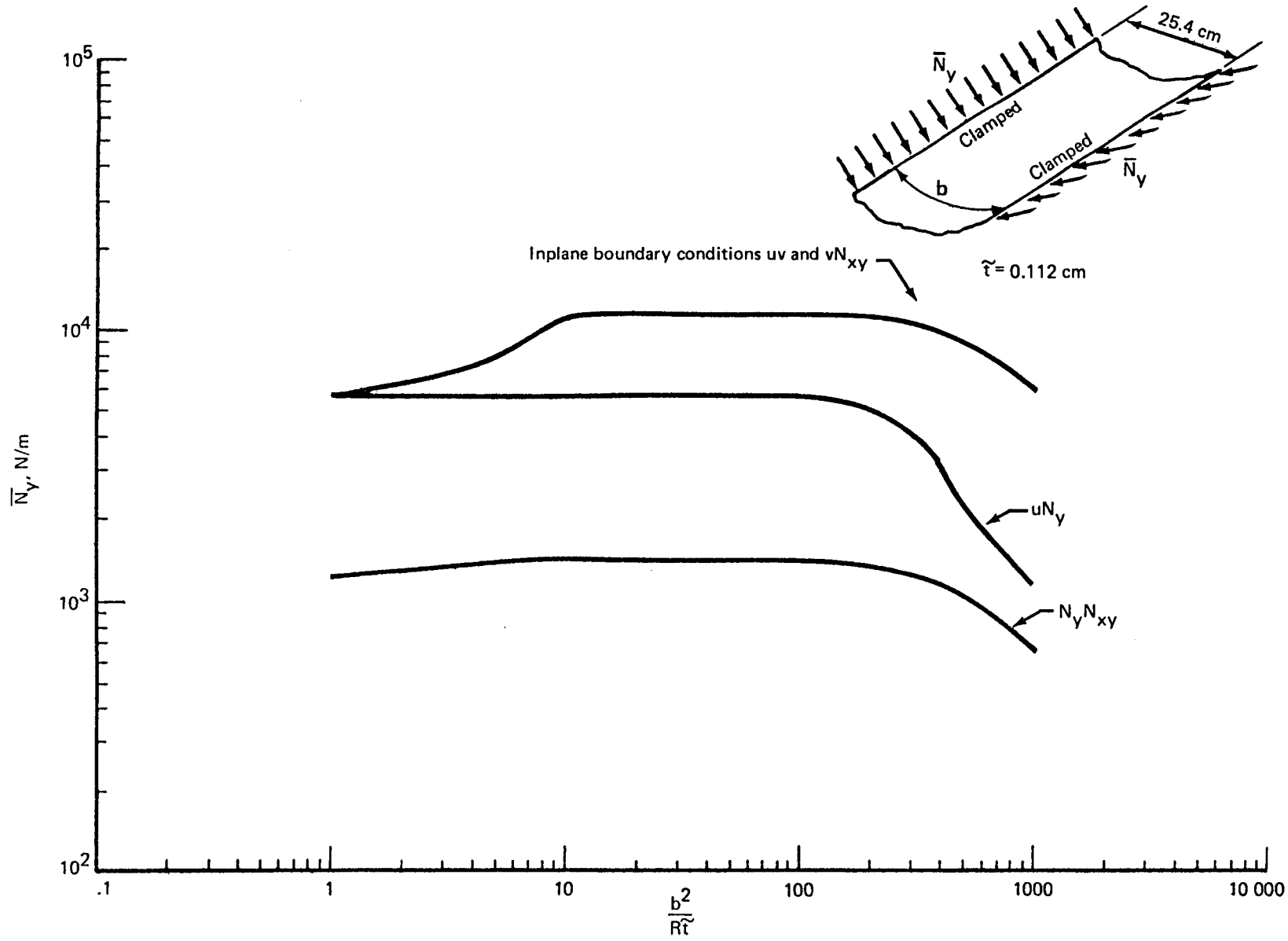

FIGURE 6.—BUCKLING RESULTS FOR CURVED LAMINATE A LOADING: $\bar{N}_y$

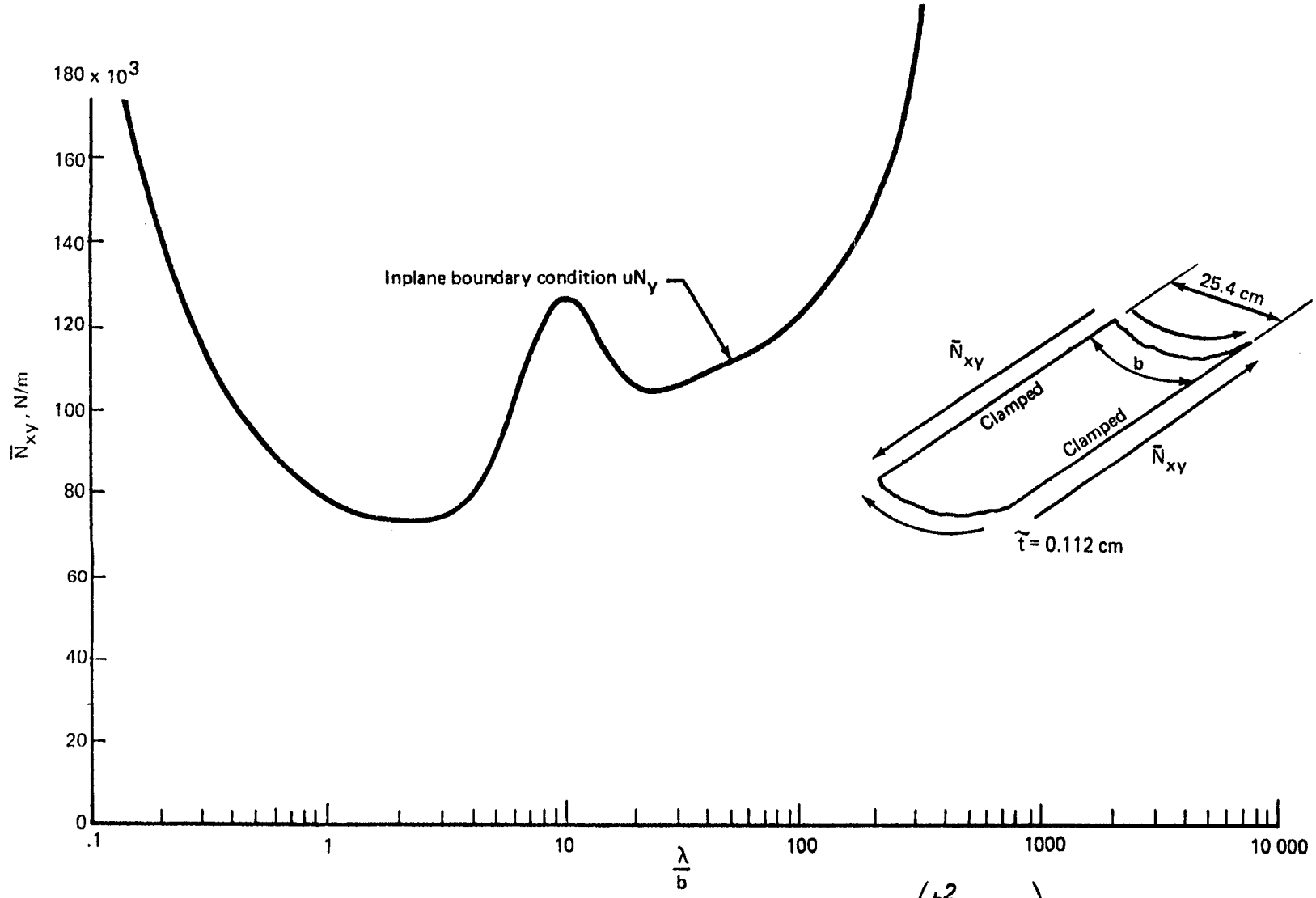

FIGURE 7.–BUCKLING RESULTS FOR CURVED LAMINATE A $\left(\frac{b^2}{R\tilde{t}} = 700\right)$
LOADING: $\bar{N}_{xy}$

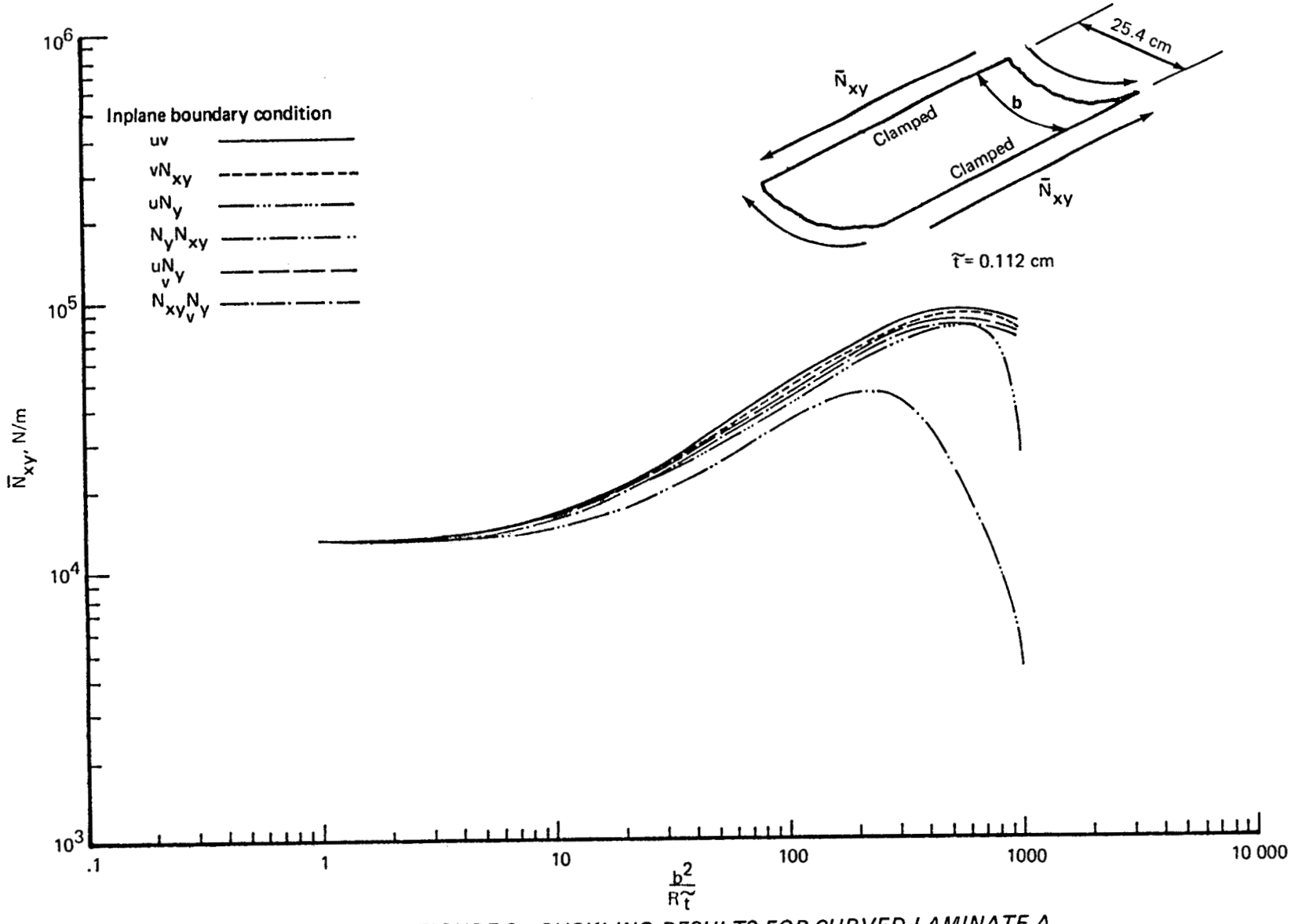

FIGURE 8.–BUCKLING RESULTS FOR CURVED LAMINATE A. LOADING: $\bar{N}_{xy}$

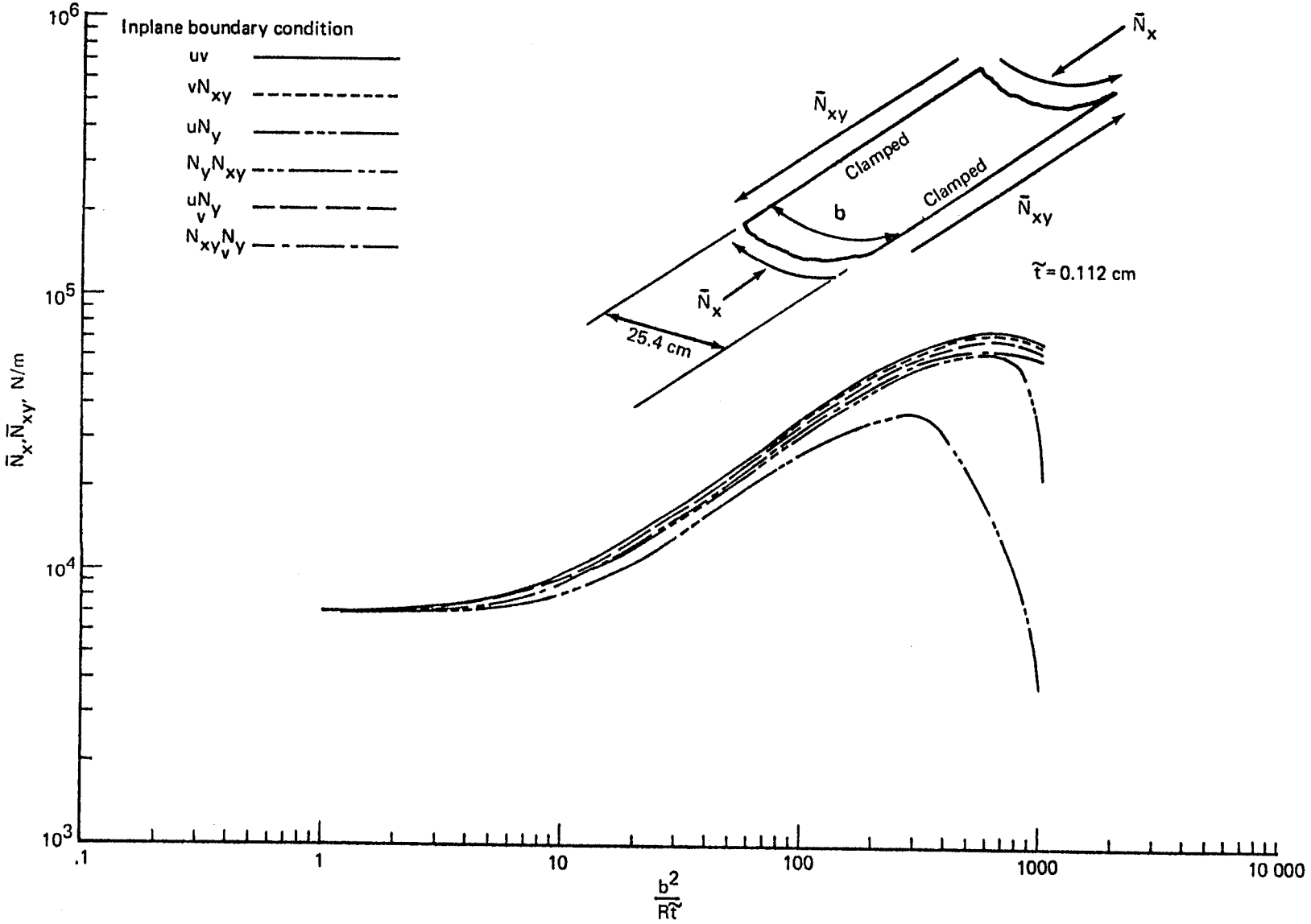

FIGURE 9.–BUCKLING RESULTS FOR CURVED LAMINATE A LOADING: $\bar{N}_x = \bar{N}_{xy}$

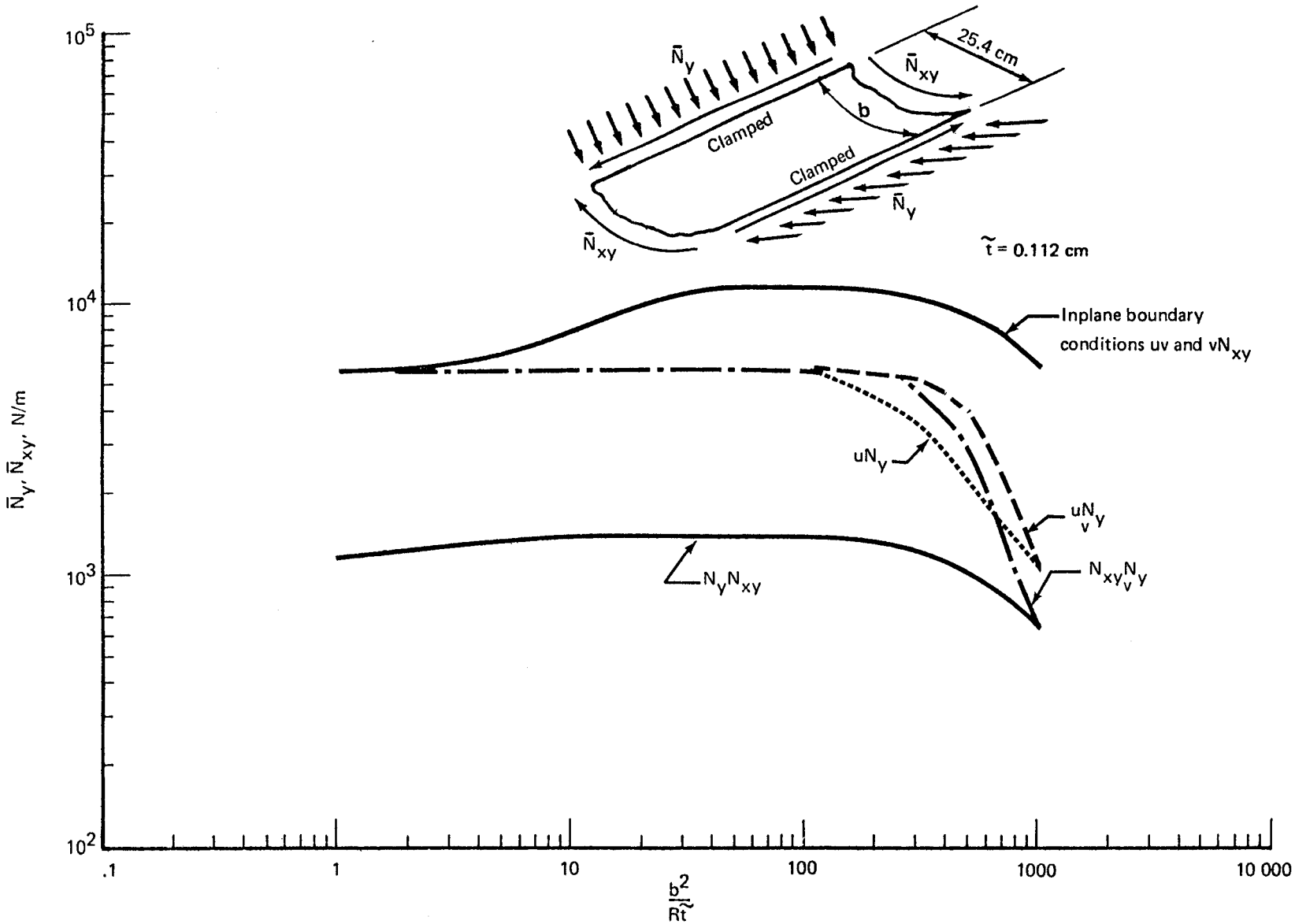

FIGURE 10.–BUCKLING RESULTS FOR CURVED LAMINATE A LOADING: $\bar{N}_y = \bar{N}_{xy}$

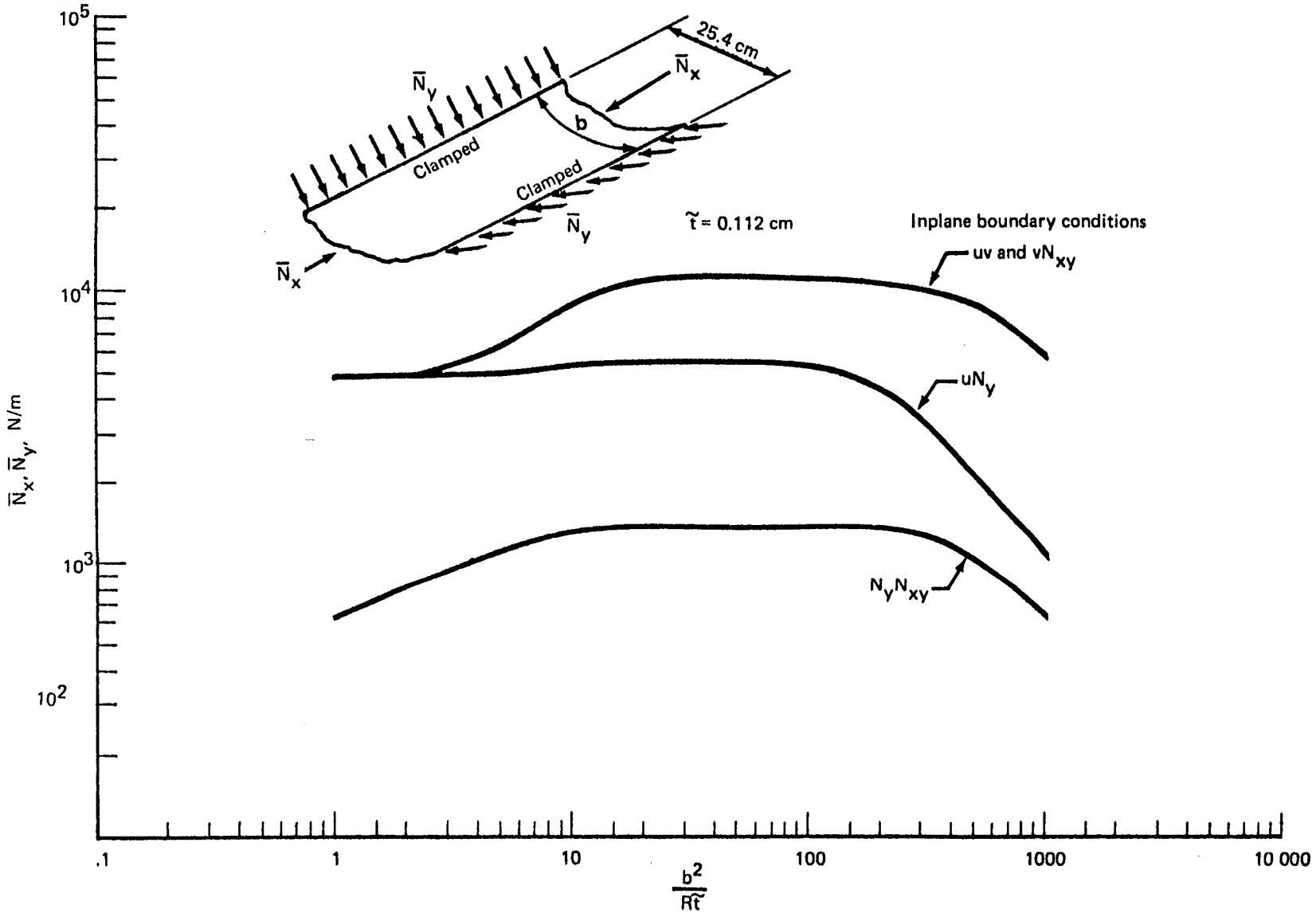

FIGURE 11.–BUCKLING RESULTS FOR CURVED LAMINATE A LOADING: $\bar{N}_x = \bar{N}_y$

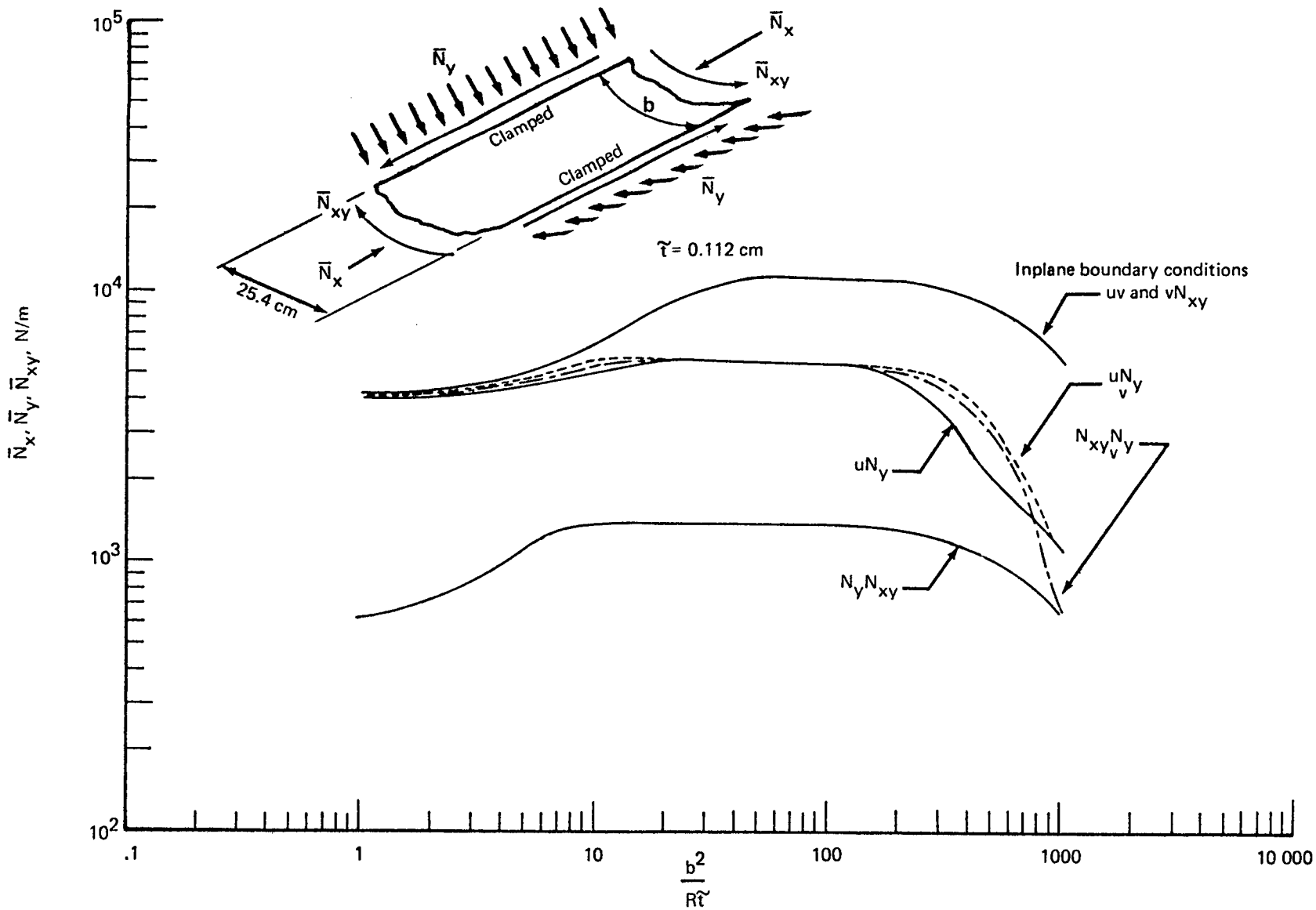

FIGURE 12.–BUCKLING RESULTS FOR CURVED LAMINATE A LOADING: $\bar{N}_x = \bar{N}_y = \bar{N}_{xy}$

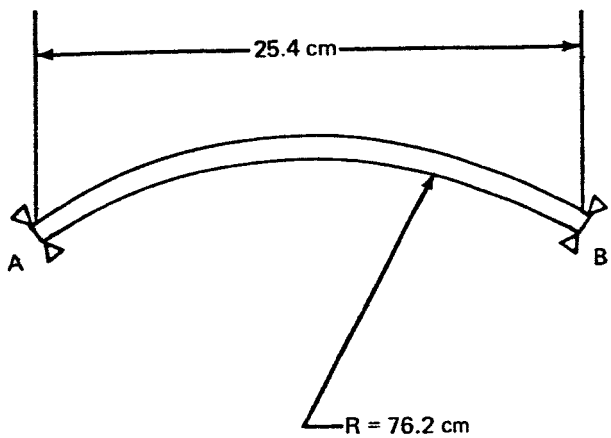

Material: boron/epoxy

Layer thickness: 0.014 cm

Boundary conditions along sides A and B:

$$w = M_y = N_y = u = 0$$

FIGURE 13.—CURVED LAMINATE B

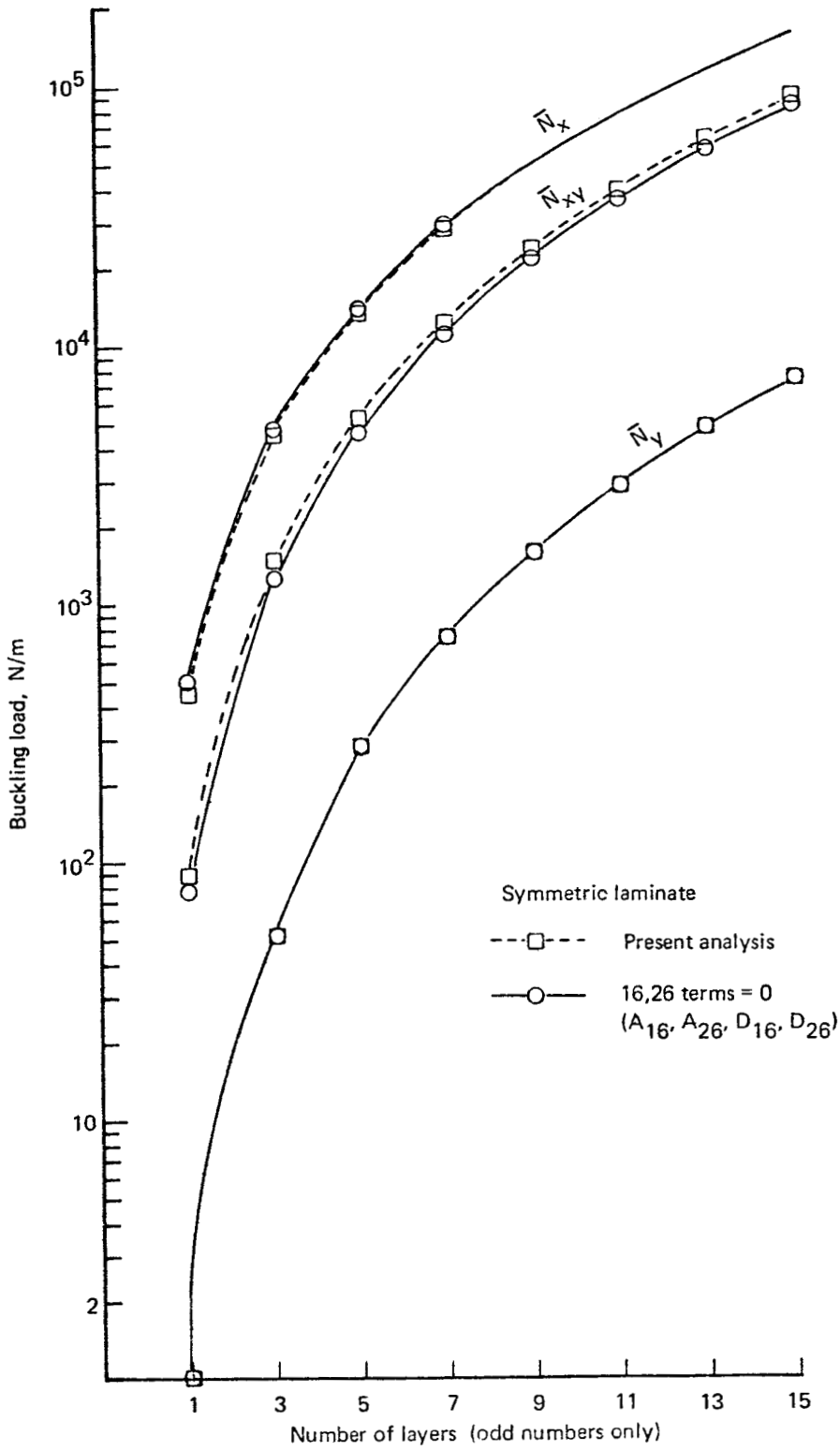

FIGURE 14.—BUCKLING RESULTS FOR CURVED LAMINATE B (ODD NUMBER OF LAYERS)

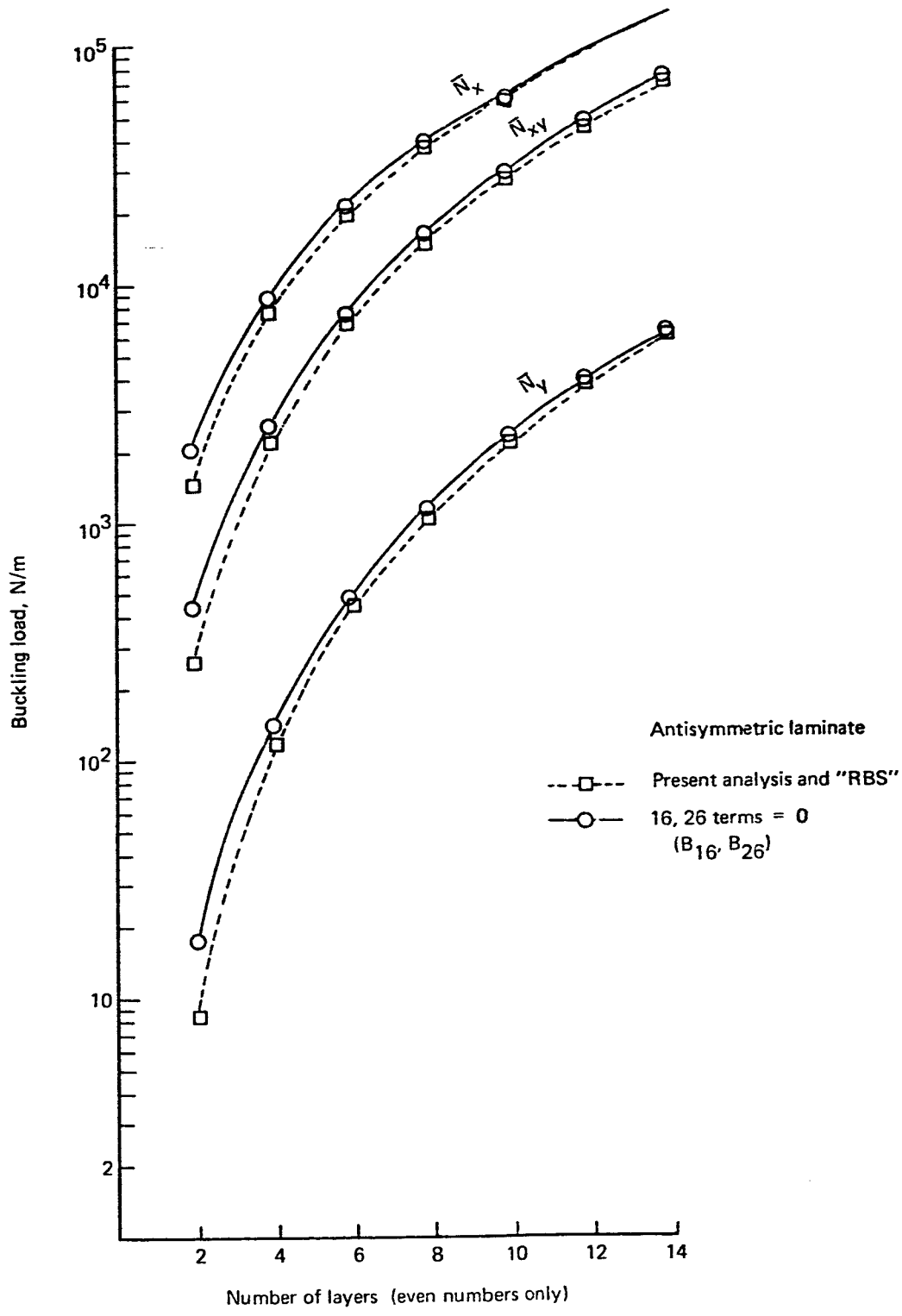

FIGURE 15.—BUCKLING RESULTS FOR CURVED LAMINATE B (EVEN NUMBER OF LAYERS)

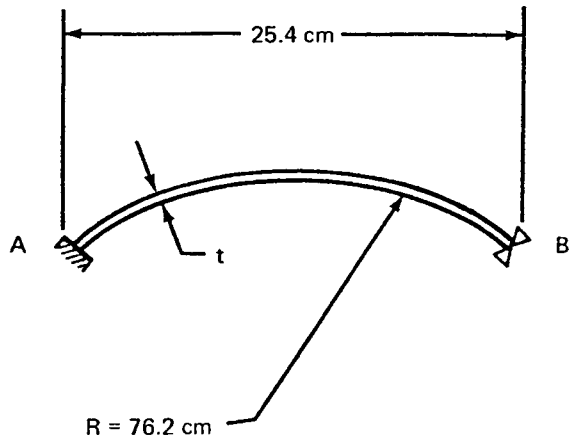

Boundary conditions along A: $w = \theta_y = N_y = u = 0$

Boundary conditions along B: $w = M_y = N_y = u = 0$

Material	Equivalent weight thickness, t, cm
Boron/epoxy	0.04267
Boron/aluminum	0.03157
High modulus graphite/epoxy	0.05334
Borsic/aluminum	0.03157
Aluminum 2024	0.03094

FIGURE 16.—CURVED LAMINATE C

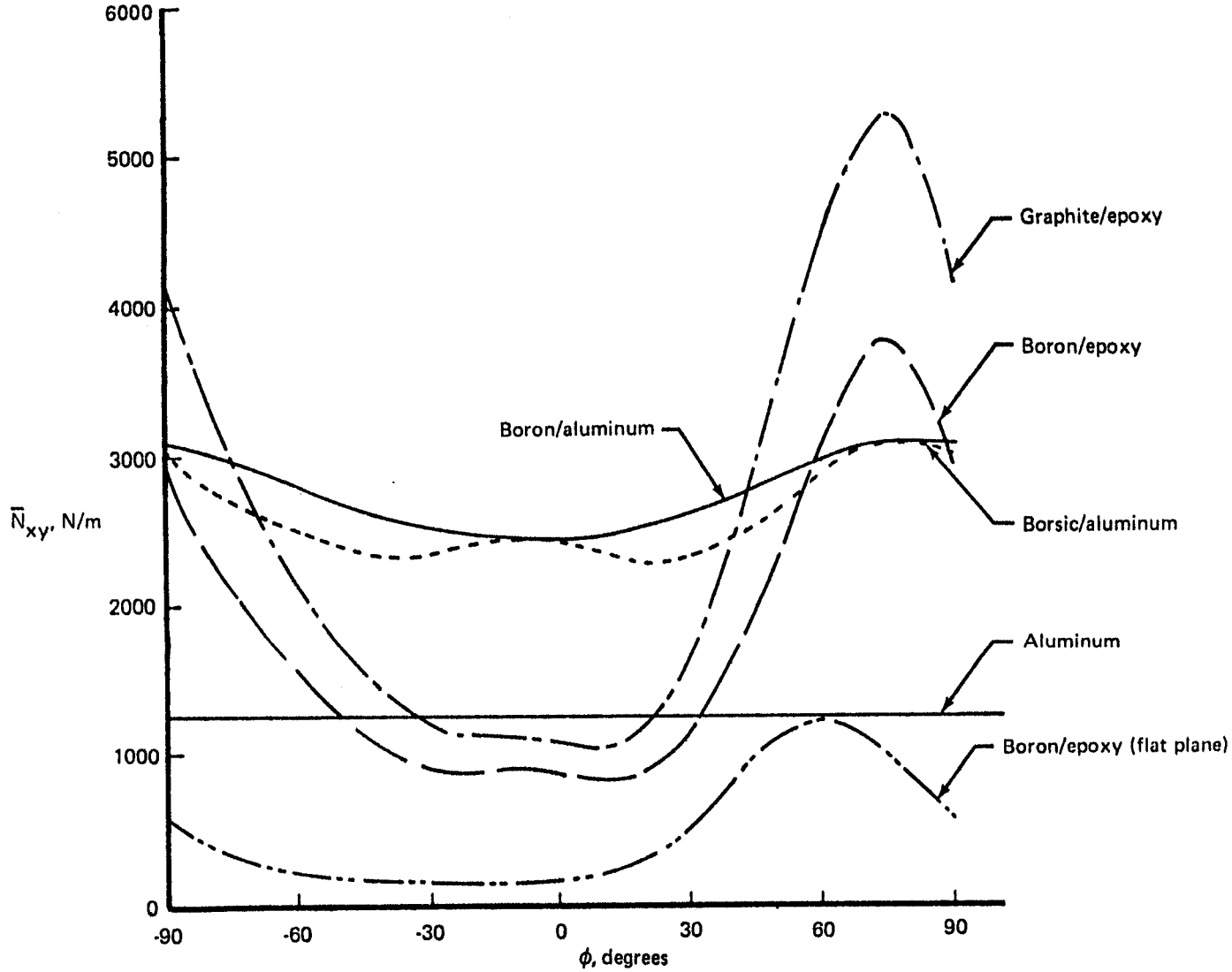

FIGURE 17.–BUCKLING RESULTS FOR CURVED LAMINATE C. LOADING: $\bar{N}_{xy}$

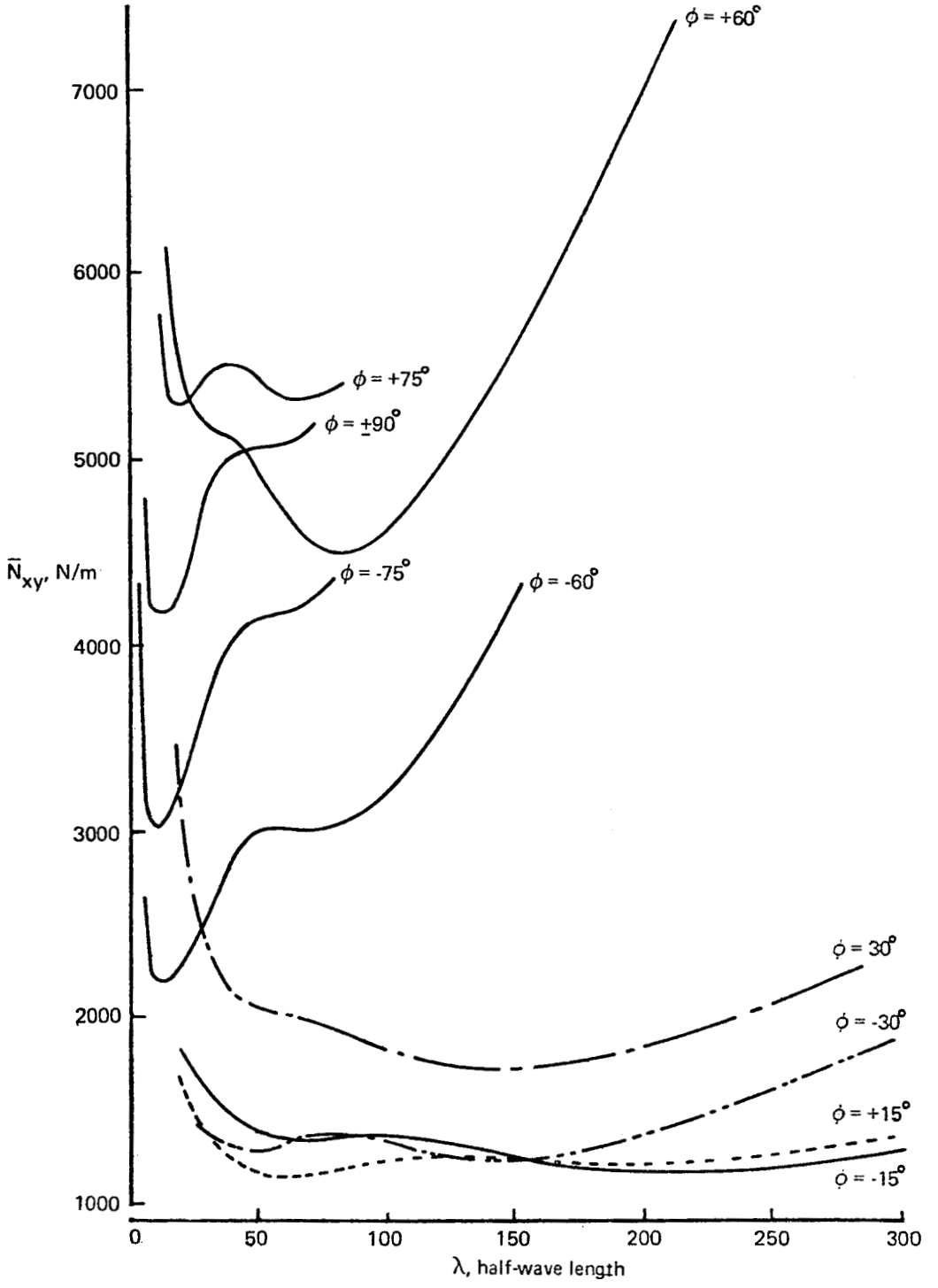

FIGURE 18.—BUCKLING FOR CURVED LAMINATE C.
LOADING: $\bar{N}_{xy}$ ONLY
MATERIAL: GRAPHITE/EPOXY

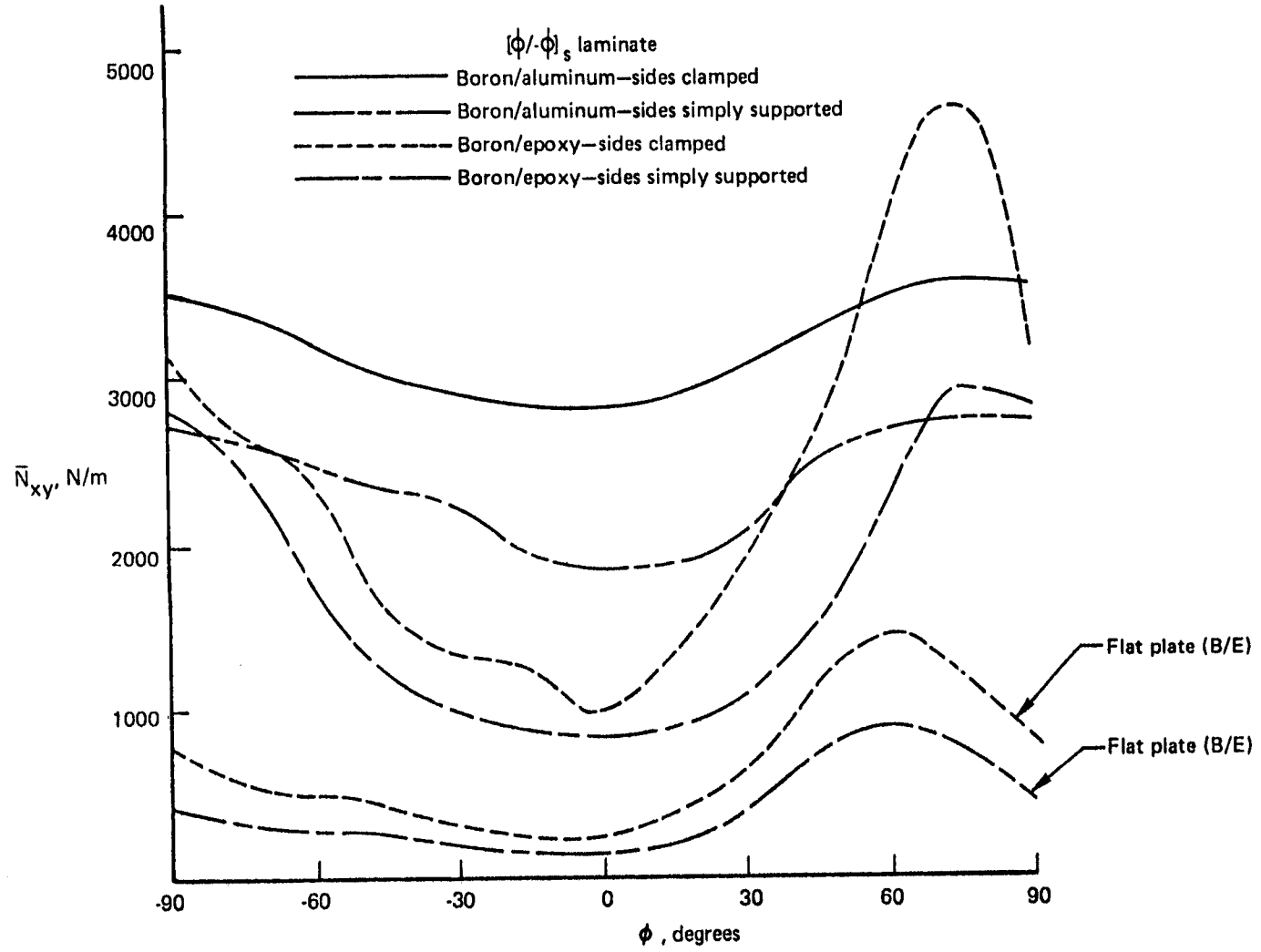

FIGURE 19.–BUCKLING RESULTS FOR AN ANGLE PLY CURVED LAMINATE LOADING: $\bar{N}_{xy}$

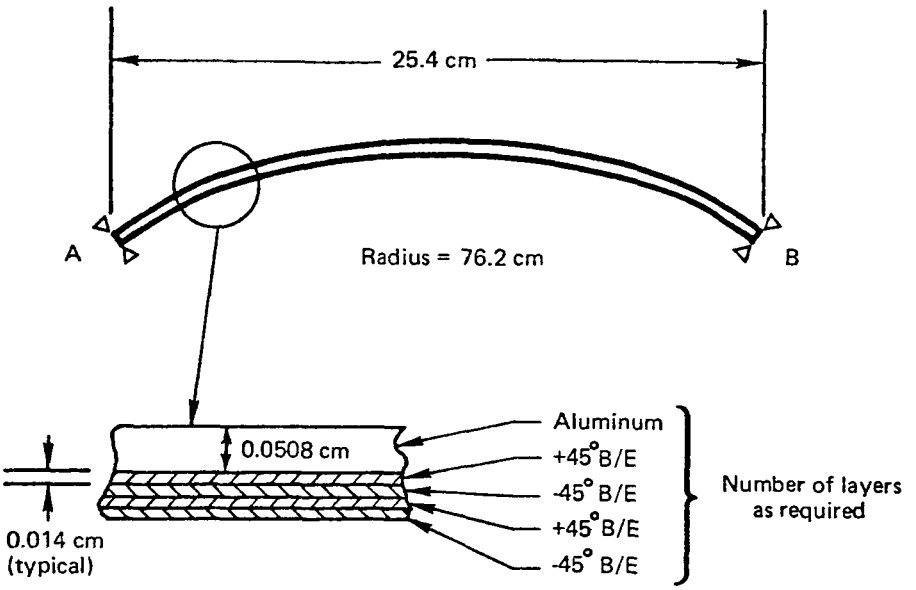

Boundary conditions along A and B:

$$w = M_y = N_y = u = 0$$

FIGURE 20.—GENERAL LAMINATE D

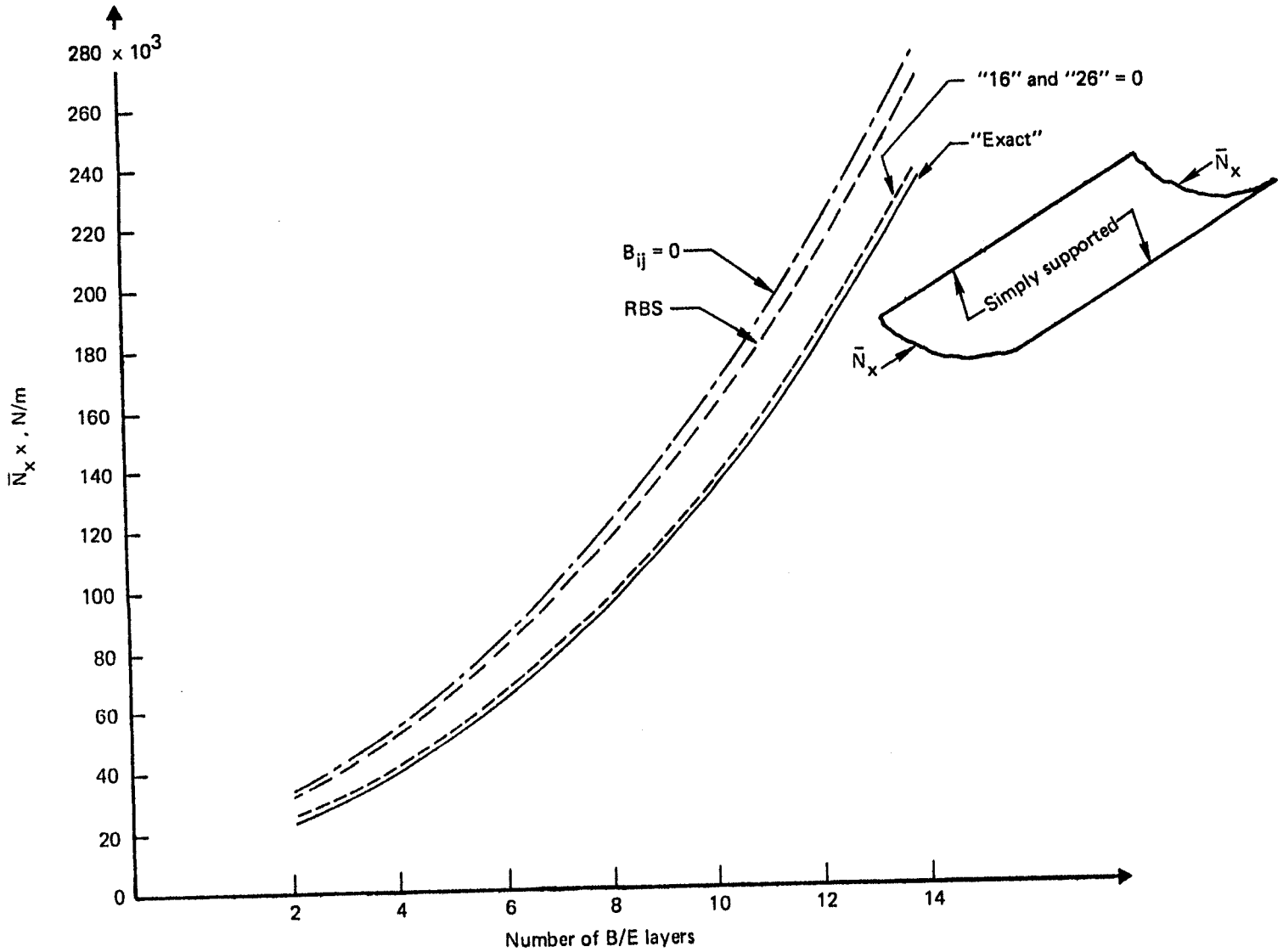

FIGURE 21.–BUCKLING RESULTS FOR THE CURVED LAMINATE D LOADING: $\bar{N}_x$

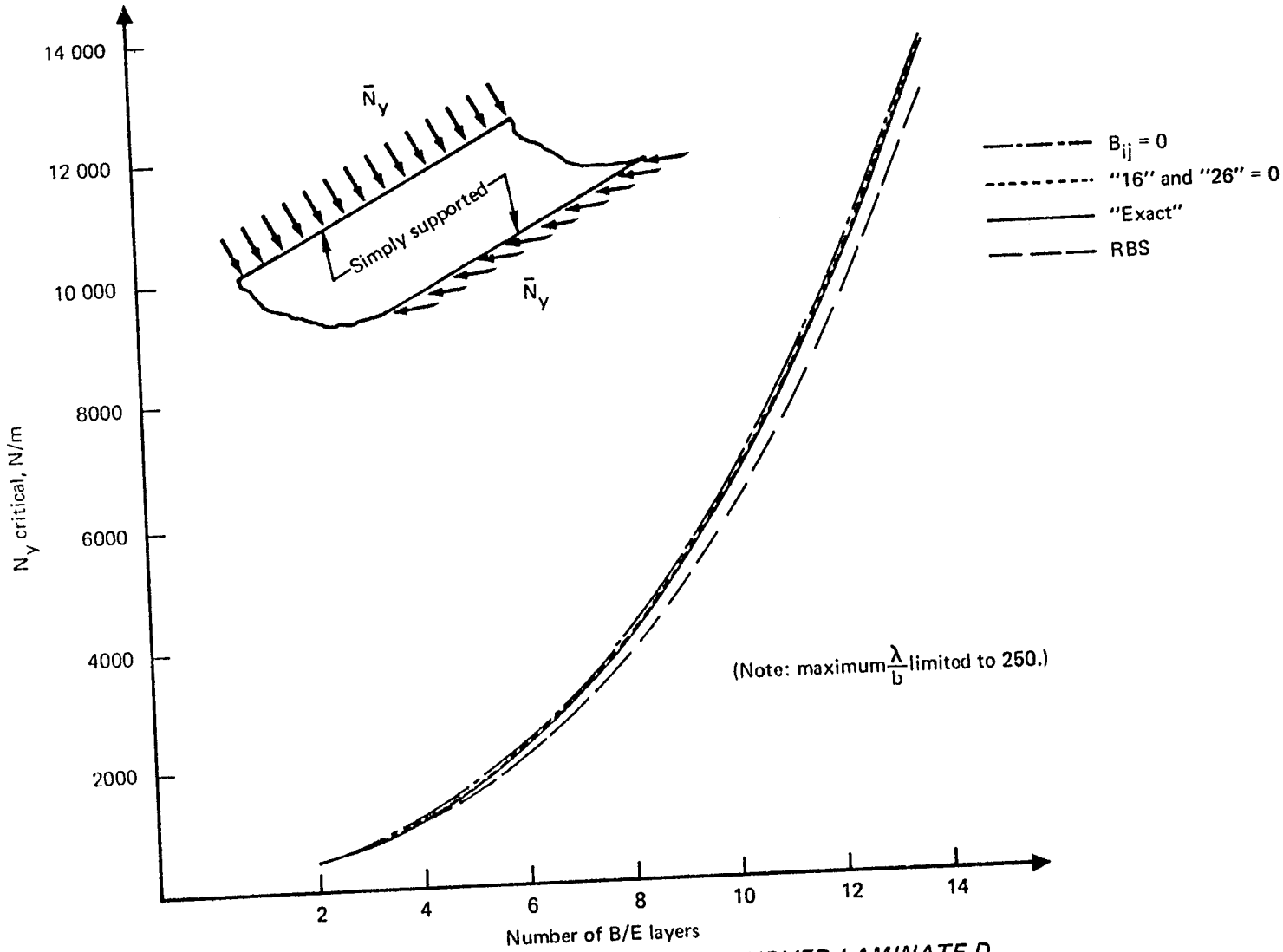

FIGURE 22.—BUCKLING RESULTS FOR THE CURVED LAMINATE D. LOADING: $\bar{N}_y$

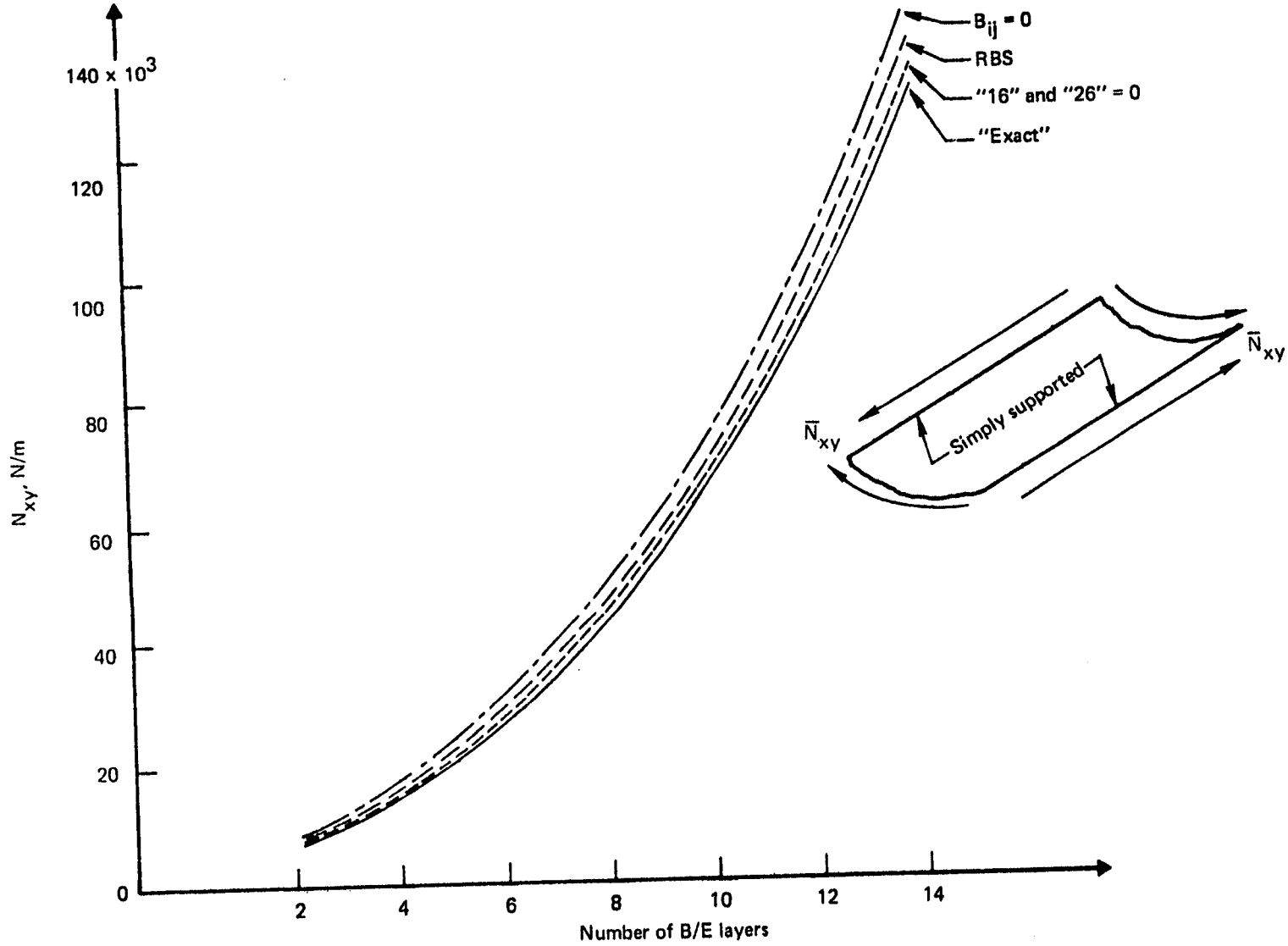

FIGURE 23.–BUCKLING RESULTS FOR THE CURVED LAMINATE D LOADING: $\bar{N}_{xy}$

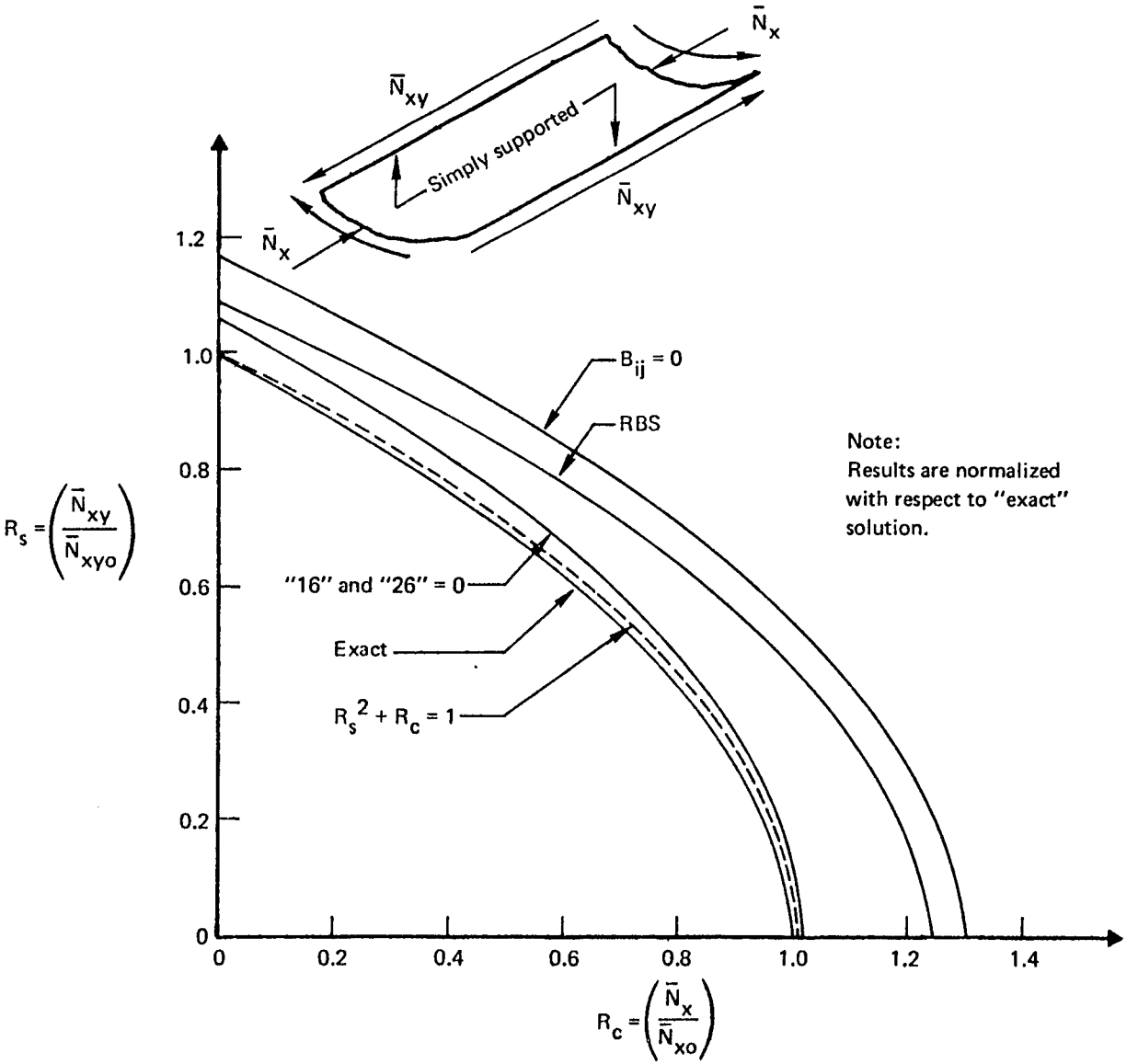

FIGURE 24.—INTERACTION CURVE FOR LAMINATE D WITH THREE [+45°/-45°] B/E REINFORCEMENT LOADING: COMBINED $\bar{N}_x$ AND $\bar{N}_{xy}$

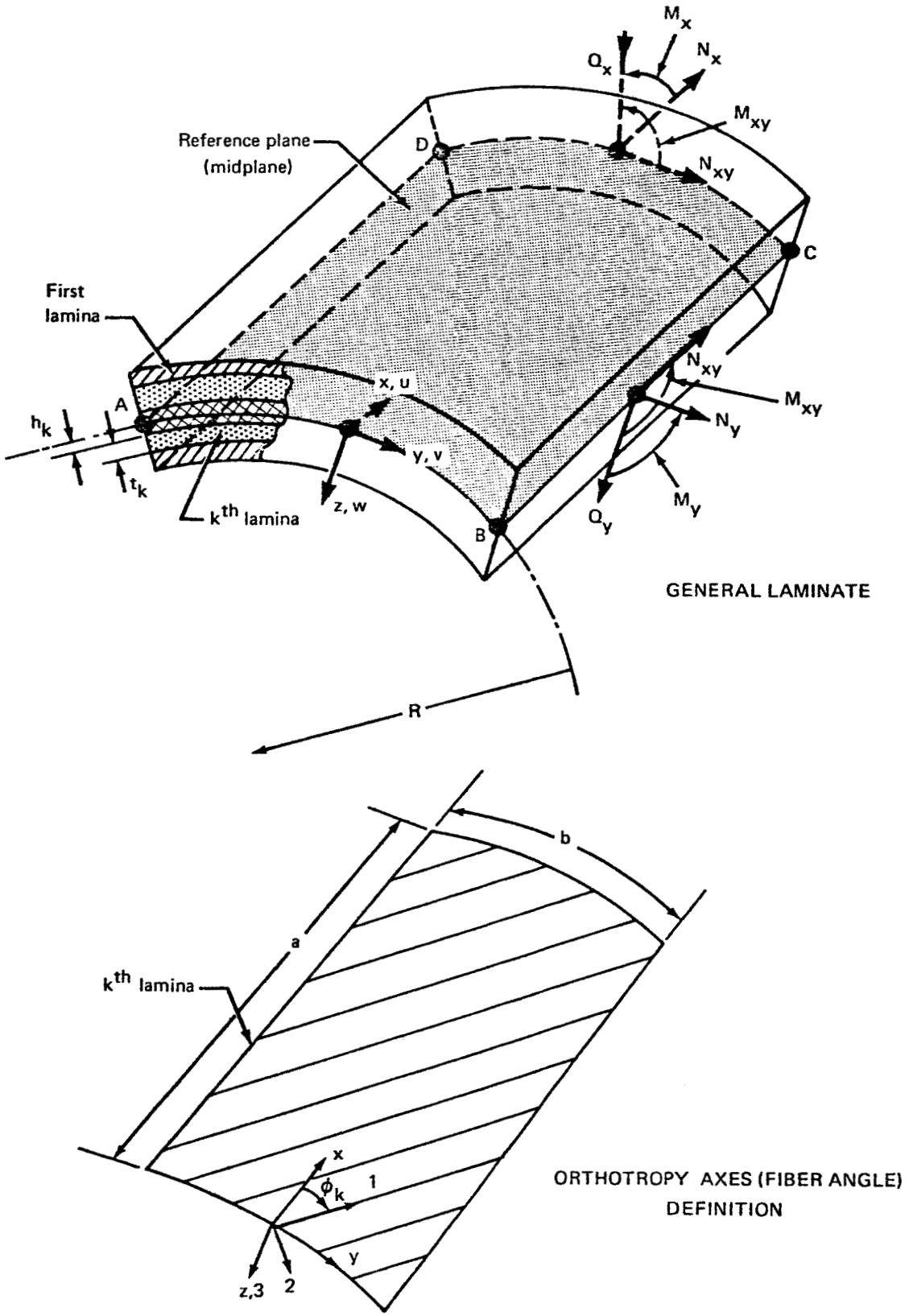

FIGURE 25.– LAMINATE GEOMETRY AND SIGN CONVENTIONS

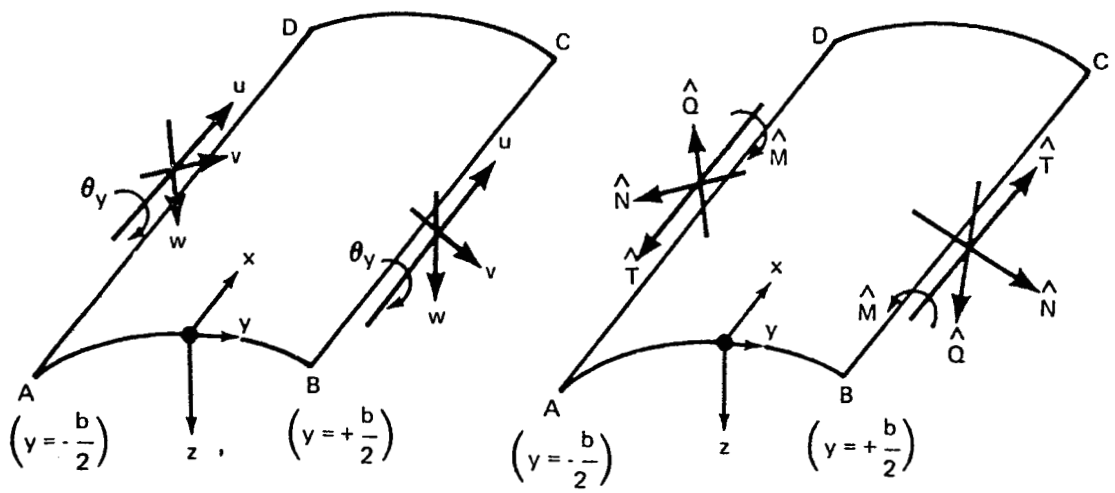

FIGURE 26.—DISPLACEMENTS AND FORCES DUE TO BUCKLING ALONG SIDES OF PLATE-STRIP

REFERENCES

1. Reissner, E.; and Stavsky, Y.: Bending and Stretching of Certain Types of Heterogeneous Aeolotropic Elastic Plates. J. of App. Mech., Sept. 1961, pp. 402-408.

2. Dong, S. B.; Pister, K. S.; and Taylor, R. L.: On the Theory of Laminated Anisotropic Shells and Plates. J. of Aero. Sciences, Aug. 1962, pp. 969-975.

3. Ashton, J. E.; and Whitney, J. M.: Theory of Laminated Plates, Progress in Materials Science Series. Vol. IV, Technomic Publication, 1970.

4. Southwell, R. V.; and Skan, S. W.: On the Stability Under Shearing Forces of a Flat Elastic Strip. Proc. of the Royal Society, Series A, Vol. 105, June 1924, pp. 582-607.

5. Batdorf, S. B.; and Houbolt, J. C.: Critical Combinations of Shear and Transverse Direct Stress for an Infinitely Long Flat Plate with Edges Elastically Restrained Against Rotation. Report No. 847, NACA, 1946.

6. Stein, M.; and Neff, J.: Buckling Stresses of Simply Supported Rectangular Flat Plates in Shear. T.N. No. 1222, NACA, March 1947.

7. Batdorf, S. B.; and Stein, M.: Critical Combinations of Shear and Direct Stress for Simply Supported Rectangular Flat Plates. T.N. No. 1223, NACA, March 1947.

8. Batdorf, S. B.; Schildcrout, M.; and Stein, M.: Critical Combinations of Shear and Longitudinal Direct Stress for Long Plates With Transverse Curvature. T.N. No. 1347, NACA, June 1947.

9. Batdorf, S. B.; Stein, M.; and Schildcrout, M.: Critical Shear Stress of Curved Rectangular Panels. T.N. No. 1348, NACA, June 1947.

10. Schildcrout, M.; and Stein, M.: Critical Combinations of Shear and Direct Axial Stress for Curved Rectangular Panels. T.N. No. 1928, NACA, August 1949.

11. Johnson, A. E., Jr.; and Buchert, K. P.: Critical Combinations of Bending, Shear and Transverse Compressive Stresses for Buckling of Infinitely Long Flat Plates. T.N. No. 2536, NACA, Sept. 1951.

12. Johnson, J. H., Jr.: Critical Buckling Stresses of Simply Supported Flat Rectangular Plates Under Combined Longitudinal Compression, Transverse Compression and Shear. J. of Aero. Sciences, June 1954, pp. 411-416.

13. Thielemann, W.: Contribution to the Problem of Buckling of Orthotropic Plates, With Special Reference to Plywood. Tech. Memorandum 1263, NACA, August 1950.

14. Gerard, G.; and Becker, H.: Handbook of Structural Stability. Part I—Buckling of Flat Plates, T.N. No. 3781, NACA, July 1957, and Part II—Buckling of Curved Plates and Shells, T.N. No. 3783, NACA, August 1957.

15. Johns, D. J.: Shear Buckling of Isotropic and Orthotropic Plates—A Review. R&M No. 3677, Aeronautical Research Council, Oct. 1970.

16. Whitney, J. M.: Shear Buckling of Unsymmetrical Cross-Ply Plates. J. of Composite Materials, Vol. 3, April 1969, pp. 359-363.

17. Whitney, J. M.; and Leissa, A. W.: Analysis of Heterogeneous Anisotropic Plates. J. of App. Mech. June 1969, pp. 261-266.

18. Chamis, C. C.: Buckling of Anisotropic Composite Plates. J. of Structural Div., Am. Soc. of Civil Engineers, October 1969, pp. 2119-2139.

19. Whitney, J. M.; and Leissa, A. W.: Analysis of Simply Supported Laminated Anisotropic Rectangular Plate. AIAA Journal, Vol. 8, No. 1, Jan. 1970, pp. 28-33.

20. Kicher, T. P.; and Mandell, J. F.: A Study of the Buckling of Laminated Composite Plates. AIAA Journal, Vol. 9, No. 4, April 1971, pp. 605-613.

21. Chamis, C. C.: Theoretical Buckling Loads of Boron/Aluminum and Graphite/Resin Fiber-Composite Anisotropic Plates. T.N. D-6572, NASA, Dec. 1971.

22. Ashton, J. E.: Approximate Solutions for Unsymmetrically Laminated Plates. J. of Composite Materials, Vol. 3, Jan. 1969, pp. 189-191.

23. Whitney, J. M.: The Effect of Boundary Conditions on the Response of Laminated Composites. J. of Composite Materials Vol. 4, April 1970, pp. 192-203.

24. Viswanathan, A. V.; and Tamekuni, M.: Elastic Buckling Analysis for Composite Stiffened Panels and Other Structures Subjected to Biaxial Inplane Loads. CR-2216, NASA, 1973.

25. McElman, J. A.; and Knoell, A. C.: Vibration and Buckling Analysis of Composite Plates and Shells. J. of Composite Materials, Vol. 5, Oct. 1971, pp. 529-532.

26. Wittrick, W. H.; and Williams, F. W.: A General Algorithm for Computing National Frequencies of Elastic Structures. Quarterly J. of Mech. and App. Maths., Vol. 24, Part 3, August 1971, pp. 263-284.

27. Halstead, David W.; Tripp, Leonard L.; Tamekuni, M.; and Baker, L. L.: A Computer Program for Instability Analysis of Laminated Long Plates Subjected to Combined Inplane Loads, Users Manual for BUCLAP2, and Program Description Document for BUCLAP2. CR-132298 and CR-132299, NASA, 1973.

28. Almroth, B. O.; Brogan, F. A.; Meller, E.; and Zele, F.: Users Manual for the STAGS Computer Code. LMSC-D266611A, Lockheed Missiles and Space Company, California, April 1972.

29. Batdorf, S. B.; Schildcrout, M.; and Stein, M.: Critical Shear Stress of Long Plates With Transverse Curvature. T.N. No. 1346, NACA, June 1947.

30. Wittrick, W. H.; and Curzon, P. L. V.: Stability Functions for the Local Buckling of Thin Flat-Walled Structures With the Walls in Combined Shear and Compression. The Aeronautical Quarterly, Nov. 1968, pp. 327-351.

31. Novozhilov, V. V.: Thin Shell Theory. P. Noordhoff Ltd., Netherlands, 1964.

32. Ashton, J. E.; Halpin, J. C.; and Petit, P. E.: Primer on Composite Materials; Analysis, Progress in Material Sciences. Vol. 3, Technomic Publication, 1969.

33. Kempner, Joseph: Unified Thin Shell Theory, PIBAL Report 566, Dept. of Aero. Engg. and App. Mech., Polytechnic Institute of Brooklyn, March 1960.

34. Novozhilov, V. V.: Foundations of the Nonlinear Theory of Elasticity, Graylock Press, 1953.

35. Duncan, W. J.: Principles of the Galerkin Method. R&M No. 1848, Aeronautical Research Committee, Sept. 1938.

36. Mechtly, E. A.: The International System of Units–Physical Constants and Conversion Factors (Revised). NASA SP-7012, 1969.